UNIVERSITY OF LEEDS

This is a repository copy of *Speciation of nitrogen compounds in the tailpipe emissions from a SI car under real world driving conditions.*.

White Rose Research Online URL for this paper:
http://eprints.whiterose.ac.uk/84627/

Version: Accepted Version

Article:
Khalfan, A, Li, H and Andrews, G (2014) Speciation of nitrogen compounds in the tailpipe emissions from a SI car under real world driving conditions. SAE International Journal of Engines, 7 (4). 1961 - 1983. ISSN 1946-3936

https://doi.org/10.4271/2014-01-2812

Reuse
Unless indicated otherwise, fulltext items are protected by copyright with all rights reserved. The copyright exception in section 29 of the Copyright, Designs and Patents Act 1988 allows the making of a single copy solely for the purpose of non-commercial research or private study within the limits of fair dealing. The publisher or other rights-holder may allow further reproduction and re-use of this version - refer to the White Rose Research Online record for this item. Where records identify the publisher as the copyright holder, users can verify any specific terms of use on the publisher's website.

Takedown
If you consider content in White Rose Research Online to be in breach of UK law, please notify us by emailing eprints@whiterose.ac.uk including the URL of the record and the reason for the withdrawal request.

White Rose university consortium
Universities of Leeds, Sheffield & York

eprints@whiterose.ac.uk
https://eprints.whiterose.ac.uk/

2014FFL--0390

Speciation of nitrogen compounds in the tailpipe emissions from a SI car under real world driving conditions

Author, co-author (Do NOT enter this information. It will be pulled from participant tab in MyTechZone)

Affiliation (Do NOT enter this information. It will be pulled from participant tab in MyTechZone)

Copyright © 2014 SAE International

Abstract

The tailpipe exhaust emissions were measured using a EURO4 emissions compliant SI car equipped with on-board measurement systems such as a FTIR system for gaseous emission, a differential GPS for velocity, altitude and position, thermal couples for temperatures, and a MAX fuel meter for transient fuel consumption. Various nitrogen species emissions (NO, NO2, NOx, NH3, HCN and N2O) were measured at 0.5 Hz. The tests were designed and employed using two real world driving cycles/routes representing a typical urban road network located in a densely populated area and main crowded road. Journeys at various times of the day were conducted to investigate traffic conditions impacts such as traffic and pedestrian lights, road congestion, grade and turning on emissions, engine thermal efficiency and fuel consumption. The time aligned vehicle moving parameters with Nitrogen pollutant emission data and fuel consumption enabled the micro-analysis of correlations between these parameters. The average data for journeys such as thermal efficiency, emissions and fuel consumption were determined. Traffic events and vehicle transient movements' impact on emissions were studied. Engine power output has been calculated by using vehicle specific power (VSP). The analysis result of tailpipe emissions and their relation to real world driving profile improved understanding of urban area nitrogen compound emissions, which will be useful for controlling of urban air quality.

Introduction

Current methods for evaluating exhaust emissions from road transport are mainly based on measurements from rolling road constant volume sampling facilities using standard drive cycles. Emissions are typically described as a function of average speed or distance for the complete cycle. The average values are subsequently used to estimate transport emissions. However, studies have demonstrated that many other parameters such as vehicle operating conditions, traffic conditions (free-flow, congested), ambient temperatures, fuel compositions, topography and road geometry strongly influence real world emissions [1-10].

Nitrogen compound from vehicle tailpipe such as NO, NO2, N2O, NH3 and HCN are toxic air pollutants (TAPs). NO is a product of combustion inside the engine. NO2 is mainly a secondary pollutant from the exhaust catalytic systems where extra oxygen is available to oxidize NO into NO2. NO and NO2 are involved in the formation of ozone (O3) in the atmosphere and able to oxidize unburned hydrocarbons to form oxygenated irritants such as formaldehyde, peroxyacetyl nitrate etc[11]. NO2 itself is an irritant air pollutant regulated by EU air quality legislation [ ]. NH3 is not a product of combustion and instead is formed across the TWC. NH3 is not directly regulated by vehicle emission legislation but is required to be monitored for the sake of the air quality, soil and surface water concerns [12]. The United Nations Economic Commission for Europe (UN ECE) has set the limits for NH3 for different European countries. However, there is no legislative requirement for NH3 released from vehicle tailpipe. NH3 can form NH3NO3 and/or (NH4)2SO4 and contribute to the formation of the secondary aerosols and is an important constituent of particulate matter (PM). NH3 has a potential to be transported over a long distance in the atmosphere and thus could potentially have adverse impacts on soil and water because of the deposition of ammonium salts which lead to acidification and eutrophication of soils and surface waters.

Heeb etc [13-15] investigated NH3 emissions and their correlation with NO emissions and concluded that catalyst temperatures and air/fuel ratios are key parameters affecting the formation of NH3 EURO 3 and 4 gasoline passenger cars. They also reported a conversion ratio of 2% to 45% for NO converting to NH3 when operating a Pd/Rh-based TWC vehicle under transient driving conditions. There is a kind of trade-off between NOx and NH3. As the NOx emission legislation is getting more stringent, more effective and efficient NOx reduction across the TWC is demanding. This may cause the rising of NH3 emissions.

Hydrogen cyanide (HCN) is a toxic air pollutant and a by-product formed during the NOx reduction reactions across the catalyst [16, 17]. There are very limited data on the HCN emissions from vehicle tailpipe being reported [17].

Nitrous oxide (N2O) is a powerful GHG (~300 stronger than CO2) and has a long life span (>170 years). The transport sector is a minor contributor to the total N2O flux in the atmosphere. However, its GWP (Global Warming Potential) could account for a notable contribution to the total GWP from vehicle tailpipe emissions. Li etc [2] investigated GWP of CO2, N2O and CH4 tailpipe emissions for five urban driving cycles and reported ~10% of the total GWP coming from N2O.

This paper investigated the tailpipe emissions of five nitrogen compounds (NO, NO2, NH3, HCN, N2O) under real world urban driving conditions during the different time of day using a EURO 4 SI passenger car. The routes used represented typical urban busy circuits including arterial and minor roads, turnings, pedestrian crossings and traffic lights. The impact of traffic conditions, road grade and vehicle's movements on these five nitrogen compounds was investigated.

Experimental

Test car and thermal measurement

A EURO4 emission compliant Ford Mondeo manual transmission petrol car was used, which was fitted with a port fuel injected 1.8 litre 16V spark ignition engine with 4 cylinders and 16 valves. The odometer reading on the car was 4,400 miles prior to the tests. The vehicle was equipped with a Three Way Catalyst (TWC). The curb weight of the car is 1374 kg. The car was instrumented with 3 thermocouples, which measured the lubricating oil in sump temperature, upstream and downstream of the TWC exhaust gas temperatures. All temperatures were measured using grounded junction mineral insulated Type K thermocouples with a response time of ~0.25 ms.

Fuel flow, air/fuel ratio, and GPS measurements

Fuel consumption measurement

A MAX710 fuel flow measurement system was used to measure real world fuel consumptions. This measured the fuel mass flow rate using a level controlled recirculation tank, transfer pump and a high-resolution flow meter. The pump maintained a constant pressure to the recirculation tank that fed fuel to the engine. This recirculation tank collected return fuel from the engine and recirculated this fuel back to the engine instead of returning it to the fuel tank. This recirculation loop allowed the use of a single meter to measure make-up fuel as it replaced the fuel consumed by the engine. Total fuel consumption was determined to better than 1% accuracy. The rate of fuel consumption was determined at a 1-second resolution. The device had an analog output, which was logged onto the second laptop computer.

Commercially available standard ultra low sulfur RON95 petrol fuel was used throughout the tests.

Air/fuel ratio

The air/fuel ratio was measured using a Horiba "Lambda Checker LD-700" in terms of lambda with a response time of 0.08 ~ 0.15 second. The LD-700 was connected to an NTK brand wide band oxygen sensor (ZrO_2 type), which was inserted into exhaust gas upstream of the TWC. The unit is calibrated for a fuel with a hydrogen/carbon ratio of 1.85 and an oxygen/carbon ratio of 0. The accuracy of the unit is ± 0.04λ for 0.91~1.19 λ and ± 0.08 λ outside this range. The LD-700 had a DC output of 0-5 volts, which was directly proportional to lambda. The DC voltage output was logged into a data logger and then into a laptop.

GPS system

A Racelogic VBOX II differential GPS system was used to provide geographical position, speed and acceleration data. The VBOX II is a GPS data logging system developed by Racelogic specifically for automotive applications. It is normally used for race track testing and other performance testing where accurate speed, position and acceleration data is required for driver performance evaluation. Data was logged at 1 Hz and stored on to a compact flash memory card, and subsequently transferred to a PC. The analogue output from the VBOX II was a 0-5V DC signal corresponding to road speed, and was fed to the data logger and then a laptop.

FTIR emission measurement system

FTIR

A portable Fourier Transform Infrared (FTIR) spectrometer was used to measure on road real world emissions. The model used was the Temet Gasmet CR 2000 which was capable of measuring concentrations as low as 0.5~3 ppm, depending on the species and applications. It has been specifically calibrated by the manufacturer to an accuracy of 2% within the calibrated measurement range, which was 20,000 ppm for CO, 30% for CO_2 and 7000 ppm for NOx respectively.

A FTIR emission measurement system was selected because of its ability to speciate VOC, $NO/NO_2/N_2O$ and measure ammonia in addition to CO, NOx, and THC emissions. The FTIR measurement for regulated emissions was calibrated against standard CVS measurement by authors using a chassis dynamometer facility and various driving cycles [18]. It was found that the FTIR measurement had excellent agreement (2% deviation) with the CVS measurement for CO_2 emissions. The N_2O and CH_4 were checked in laboratory using bottled gases and found good agreements as well.

The Temet instrument comprised a FTIR analyzer, a portable sample handling unit (filtering and controlling sample flow), heated sample lines and a laptop. The system weighed approximately 30 kg. The entire on-board measurement instrumentation including the FTIR system, the fuel consumption measurement system, two batteries and a DC-AC converter weighed approximately 150 kg.

The software of the FTIR system has the additional capability of accepting analog inputs, which can be logged together with the emissions spectra and analysis data. One of these analog input channels was employed to log one or two external analog signals for time alignment between the FTIR laptop and the second laptop. The voltage output from the VBox was used as the external signal and exported to two laptops: One for the FTIR that logs emission spectra and external analog signals; the other one for temperature measurement and fuel meter logging.

Power for instruments

The power needed for the on-board measuring system was around 1200 Watts and this would have necessitated drawing up to 100 A at 12V from the car's electrical system. This would have required an upgraded alternator and increased the load on the engine, therefore affecting the emissions characteristics. Another possibility was to use a small dedicated generator but this option is only feasible in large heavy duty vehicles. Therefore, a dedicated power supply, two 12V battery packs and an on-board DC-AC converter, were used to provide 240V AC necessary for instrument operation. The two batteries used weighed a total of 70 kg. They provided approximately 2-3 hours of operation before needing recharging.

Sample conditioning

In order to measure wet concentration, the raw undiluted sample gas extracted from the exhaust system had to be maintained at about 180℃ otherwise low boiling point pollutants would drop out due to condensation. Furthermore, the extracted exhaust sample had to be hot filtered so that the sample cell remained free of particulates which would contaminate it and shorten its lifetime. A sample handling unit was acquired to perform these functions. The sample handling unit uses a pump to continuously extract sample from the vehicle's exhaust system at a constant flow rate (2~3 l/min) via

a heated line. This is then filtered using a 0.2 µm filter and introduced via another heated line into the sample cell of the FTIR. Both heated lines were maintained to 180℃ by the sample handling unit. The sample handling unit consumed the most power since it performed heating and pumping functions. It was installed in the boot of the car along with the FTIR. The gas sample was taken downstream of the catalyst and the heated sample line was passed through a small hole in the car's floor pan. There was no possibility of dilution of the sample by pressure pulsations from the tailpipe.

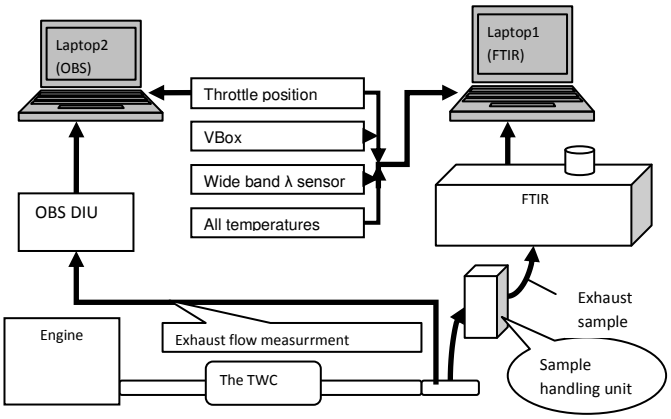

Figure 1: Schematic view of sampling and data logging system

Mass emission and VSP calculation

Mass emission calculation

The FTIR emission measurements were on a volumetric basis. These were converted into a mass basis using the conventional method for the computation of emissions index (EI: g/kg fuel)

$$EI = 1000*K*C*(1+A/F) \text{ g/kg fuel} \quad (1)$$

Where

- K is conversion coefficient, which is the ratio of molecular weight of a certain emission component to the molecular weight of the whole sample gas. The molecular weight of the exhaust sample gas is close to that of air and does not vary more than 1% for H/C ratios of about 2 (i.e. gasoline), irrespective of the air/fuel ratio. For this reason, K is here treated as a constant.
- C is concentration of the component. If this is measured in ppm or % then the equation has to be multiplied by 10^{-6} or 10^{-2} respectively.
- A/F is the air/fuel ratio on a mass basis measured by lambda sensor.

The EI was then converted into mass emission rate g/s using fuel consumption measured for the sampling period. Then the distance based emissions can be calculated for any distance traveled.

Vehicle Specific Power (VSP)

The generic VSP estimation equation was used with the typical coefficient values for a light-duty vehicle [19].

$$VSP = v*(1.1*a+9.81*\sin(\text{atan}(\text{grade})) +0.132)+ 0.000302*(v)^3 \quad (2)$$

Where:

- v is vehicle speed (m/s)
- a is vehicle acceleration (m/s^2)
- grade is road grade, = vertical rise/horizontal distance (dimensionless)

VSP is defined as the instantaneous power per unit mass of the vehicle, with units of kilowatts per tonne (kW/tonne).

Test route and procedure

Two urban driving cycles were designed to carry out emission tests: Headingley route A and route B, referred as route A and B hereafter. Figure 2 shows the map of the routes. Headingley is a dense residential area in Leeds and has a feature of typical urban road network, i.e. carrying numerous city social-economy activities and being one of the main transportation carriers.

The test trips started from point 1 in figure 2, a side road, enabling preparation of instruments and then turned right to join one of the city's major roads A660. The probe vehicle passed a pedestrian crossing and travelled towards point 2, where the route A and route B differed. Figure 3 shows the different movement at point 2 for two routes. For the route A, the vehicle went straight through the junction and travelled to point 3 and then took a U-turn moving back towards point 2. At the junction the vehicle took a right turn and moved towards point 4 and then took the second U turn travelling back to point 2. The vehicle turned right at point 2 back to A660 and travelled back to point 1. For route B, the vehicle coming from point 1 took a left turn at point 2 and travelled up to point 4 and then had a U turn moving back to point 2. The vehicle turned left at point 2 and continued to travel to point 3, where a U turn is taken and the vehicle was back to point 2 along A660. The vehicle was then straight travelling through the junction at point 2 and moved back to point 1.

There are 4 pedestrian crossings and three sets of junction traffic lights in this urban road network. Though the testing routes were a return trip but did not pass all these crossing and traffic lights. The topography of the road is not flat and thus uphill and downhill travels are experience. The real time elevations of the probe vehicle were logged by on-board GPS system and were validated by the ordnance map and the final corrected elevation data was plotted in all diagrams.

The distance traveled for each trip is ~5 km The speed limit on these urban streets is 48 km/h (30 mph)

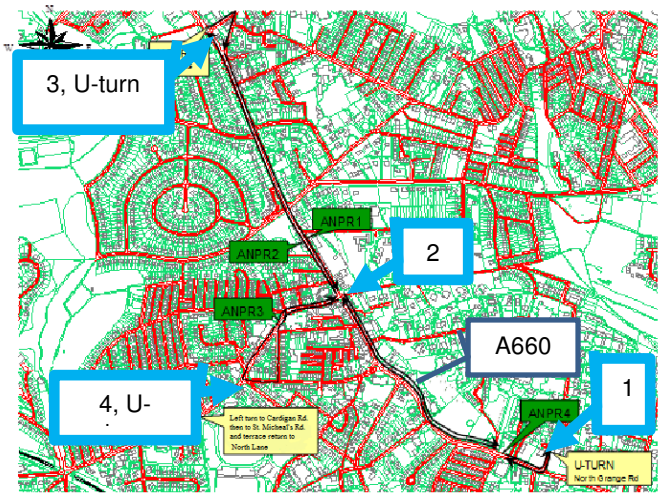

Figure 2: Map and notations of driving route.

Figure 3: Different maneuver at point 2 for Route A (left) and B (right)

Results and discussions

Driving parameter analysis - Velocity and acceleration

Figures 4 to 7 and 8 to 11 show the profiles of four A trips and four B trips respectively, including vehicle's velocity, acceleration, transient and cumulative fuel consumption, Transient VSP and cumulative power output, elevation of road, distance travelled, lambda and concentration of HCN, NH_3, NO_2, NO, N_2O in ppm. The important milestones for the trip are marked on the elevation diagrams of figures 4-11. The notes are R for right turn, L for left turn, P for pedestrian crossing and T for traffic light.

The trip A can be divided into two directions: outwards and inwards section towards city center. The first 2.0 km was the outward trip. The inwards trip towards city center is about 2.5 km except figure 5 where the logging of instruments finished earlier due to technical problems. It can be found in the figures 4a to 7a that the outbound journeys for two morning ones and lunch time one took approximately 300 seconds whereas the one in evening (figure 7) took ~250 second, indicating less traffic in the evening. The velocity and acceleration profiles show that outbound journeys were less congested than that of inbound journeys. There were one to two stops for the outbound journeys but in general there was a chunk of time when the vehicle was in cruise mode. The inbound journeys however, were much more congested, indicated by more stops and longer idling times. This was particularly obvious for two morning trips as they were in morning rush hours. The evening trip (figure7) was much less congested as this was off-peak time.

Figures 8 to 11 show the profiles of four B trips. For trip B, the outbound section was approximately 3 km, leaving a 2 km for inbound section. Two morning B trips show different traffic scenarios. 8:07 B trip in Figure 8 show that this outbound journey took approximately 550 seconds and was relatively not very congested whereas the outbound journey in figure 9 (8:53 B trip) took about 750 seconds and was a very congested section. In contrast, the inbound journey in figures 8 and 9 showed opposite trend, the one in figure 8 was very congested compared to the one in figure 9. This can be explained by the time. The journey in figure 9 started at 8:53 and when the vehicle reached to the U turn point 3 and started travelling back towards city center, it was about 9:05. The traffic was getting calm by this time as most of the commuters were needed to get to work by 9 am. Figure 10 (13:16 trip B) shows that there was some congestion in outbound direction during the noon. This was common as this is a congested road (A660) for most of the time of the day. Figure 11 shows that in off-peak time the journey (19:41 trip B) was much smooth with much of the time in cruise mode.

VSP represents the power required from the engine to move a vehicle to overcome the aerodynamic drag, rolling resistance and the road grade effect. The value of VSP is mainly determined by acceleration and road grade. If the vehicle is travelling on a flat or downhill road at a constant speed, the value of VSP would be small as the power demand will be low. This can be illustrated with examples 40-100 s in figure 4 (7:46 trip), 50-100 s in figure 6 and figure 11. The most dominant factor for VSP is acceleration, evidenced by that most of negative VSP spikes are linked with deceleration peaks.

The average of overall VSP and positive VSP for all trips presented in appendix A shows that the two evening trips had the higher values as a results of more free flow driving. The morning trips had lower values. This means that the average VSP could be used an indication for congestion. From this study, an initial suggest is that average VSP 1.4 or average positive VSP 3.1 could be used as indication for a non-congested trip.

Concentration of nitrogen compounds

The detection limits of the FTIR for these five nitrogen compounds are around 2~3 ppm. The results show that in the morning rush hour and midday HCN and NO2 concentrations were above detection limits (figures 4,5,6,8,9,10) whereas for the two evening trips (figures 7 and 11), HCN and NO2

concentrations were generally below the detection limits. NH3 and NO concentrations were higher than the detection limit for all the trips. N2O concentrations were overall below or close to its detection limit.

Time resolved mass emissions

Figures 12 to 19 show the mass emission rate (g/s) and cumulated mass emissions for five nitrogen compounds as a function of time, along with some driving parameters. NH3 is the most abundant nitrogen compound emitted from the exhaust gases and has a value of 0.05~0.09 g/km. Bielaczyc etc [20] investigated NH3 emissions from EURO5, 4 and 3 emission compliance SI passenger cars using the NEDC test cycle. They reported much lower NH3 emissions from all three vehicles. Table 1 compared NH3 emissions from Bielaczyc work with this research. The make and model of the EURO4 passenger car in Bielaczyc's paper is unknown and therefore direction comparison may be difficult as the tailpipe NH3 emissions may be related to type of the TWC. However, the gap between their results from NEDC and the real world driving cycle in this research is too large to be attributed to the possible difference in catalyst technology and type. The frequent stop and start, much harsher acceleration and deceleration, greater and more transient power demands for engine under real world driving conditions presented in this paper are important parameters causing high tailpipe NH3 emissions. Karlsson etc [17] compared NH3 emissions from NEDC and UDC (Urban Driving Cycle) of FTP-75 and observed a much higher NH3 emissions from UDC than NEDC due to harsher accelerations in the UDC. This is in a good agreement with this paper's finding, i.e. rapid and harsh accelerations are the main causes of NH3 emissions.

The peak NH3 emission rate (g/s) from eight trips in figures 12-19 are generally in the range of 2~3 mg/s, well aligned with the reported data from Heeb etc [15] using the German highway cycle (BAB).

Table 1: Comparison of NH3 emission (mg/km) from reference [20] and this research

	EURO 5 (ref)	EURO4 (ref)	EURO3 (ref)	EURO4 (this paper)
NEDC	5.27	2.91	16.52	
UDC	6.7	4.13	19.21	
EUDC	4.46	2.2	14.99	
Leeds-Headingley cycle				50~90

The peak mass emission rate of HCN was generally around 2 mg/s. The distance based HCN emissions were 5~15 mg/km between the eight trips. These values are significantly higher than those using Euro 1 and 2 SI cars and close to the values of a high mileage pre-Euro SI car reported by Karlsson etc [17]. The high HCN emissions from the Euro4 SI car may be related to the high NH3 emissions as both are by-products of de-NOx reduction reactions across the TWC. However, the detailed mechanism on the formation of HCN through the TWC is not clear.

The NO2 emissions are generally low for all the trips but the fraction of NO2 in NOx is higher than those generally recognized values [15], which were <1%. The possible reasons for this are that the journeys presented in this paper were mostly congested and thus have more decelerations (lean spikes), which resulted in further oxidation of NO.

N2O is usually formed when the TWC temperature is at certain ranges (250~350 C). The TWC temperature was not measured but the downstream of TWC gas temperature was measured in this research, which can be used an indirect indication of the TWC temperature. The downstream of TWC temperatures were above 450C in 7 out 8 journeys, except the journey in figure 9. The N2O emissions had an initial spike for all the journeys after the engine started. However, there were hardly any obviously detectable N2O emissions during the trips. This indicated that when the catalyst temperature was hotter than 450 C, N2O formation across the TWC was trivial. There is a clear N2O concentration spike in figure 9 at around 360 s, where the catalyst temperature is about ~400 C. This means that the ceiling of the temperature window for the formation of N2O could be around 400 C.

All the nitrogen compound emissions are related to the accelerations and positive VSP, even when there was no lambda deviation from 1. But not all the accelerations produce emission spikes.

Distance based cumulative mass emissions

Figures 20 to 27 show the cumulative mass emission (g) as a function of the distance travelled for five nitrogen compounds. One of the main purposes for these diagrams is to illustrate the effect of pollutant accumulation on the congested traffic. The longer the vehicle stands still, the higher the accumulated emissions. All the major step rises in any emissions are linked to stoppages of the vehicle. As the traffic lights, pedestrian crossings, left or right turns are marked in the diagrams, the accumulation of pollution can then be determined.

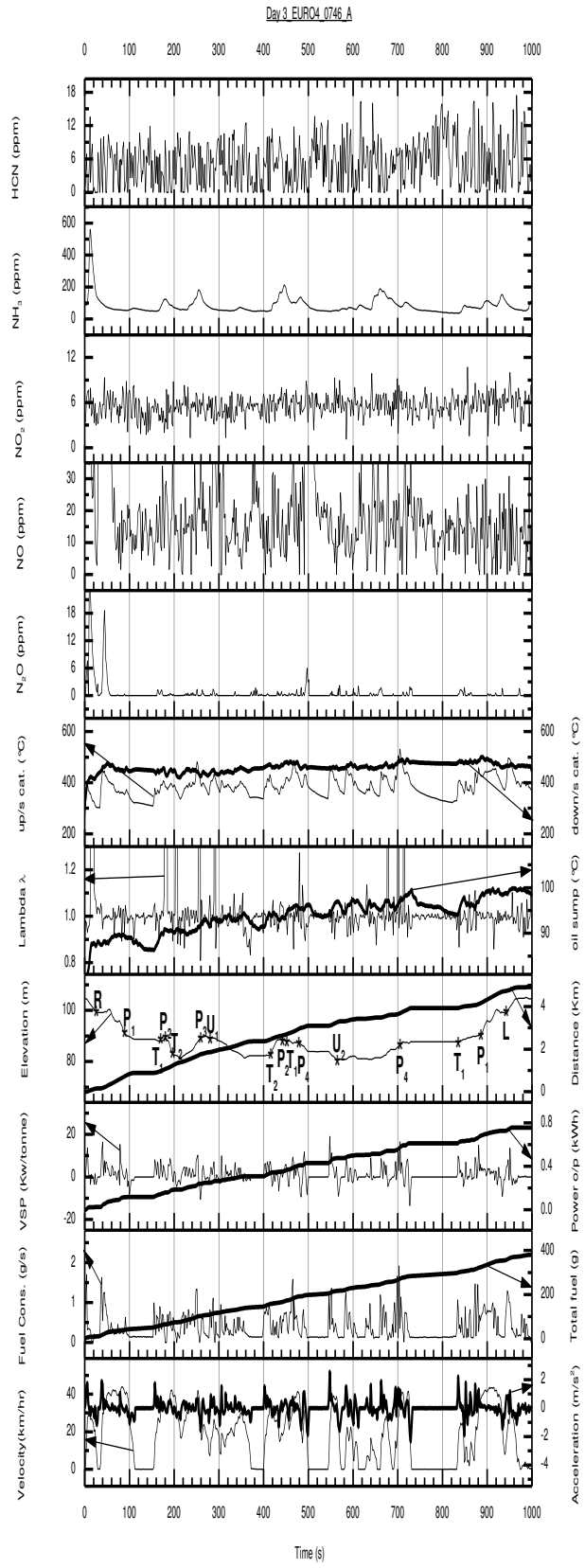

Figure 4: Profiles for the trip 7:46A-a

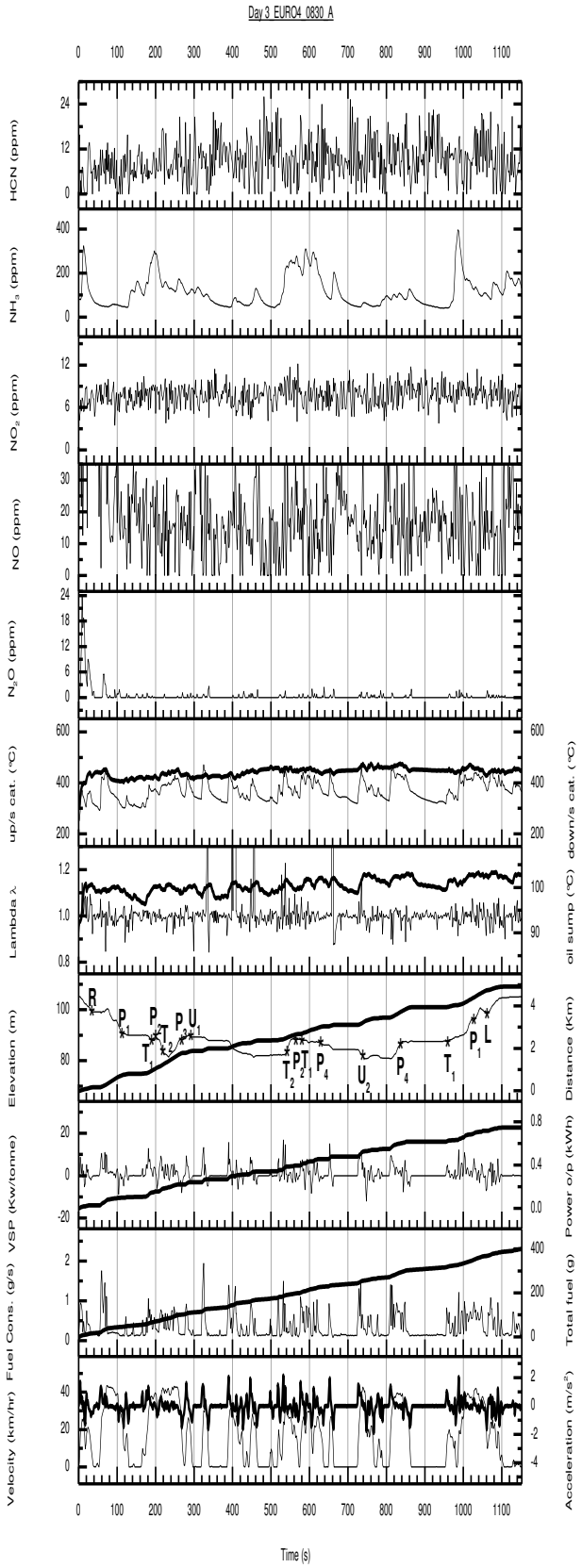

Figure 5 Profiles for the trip 8:30A-a

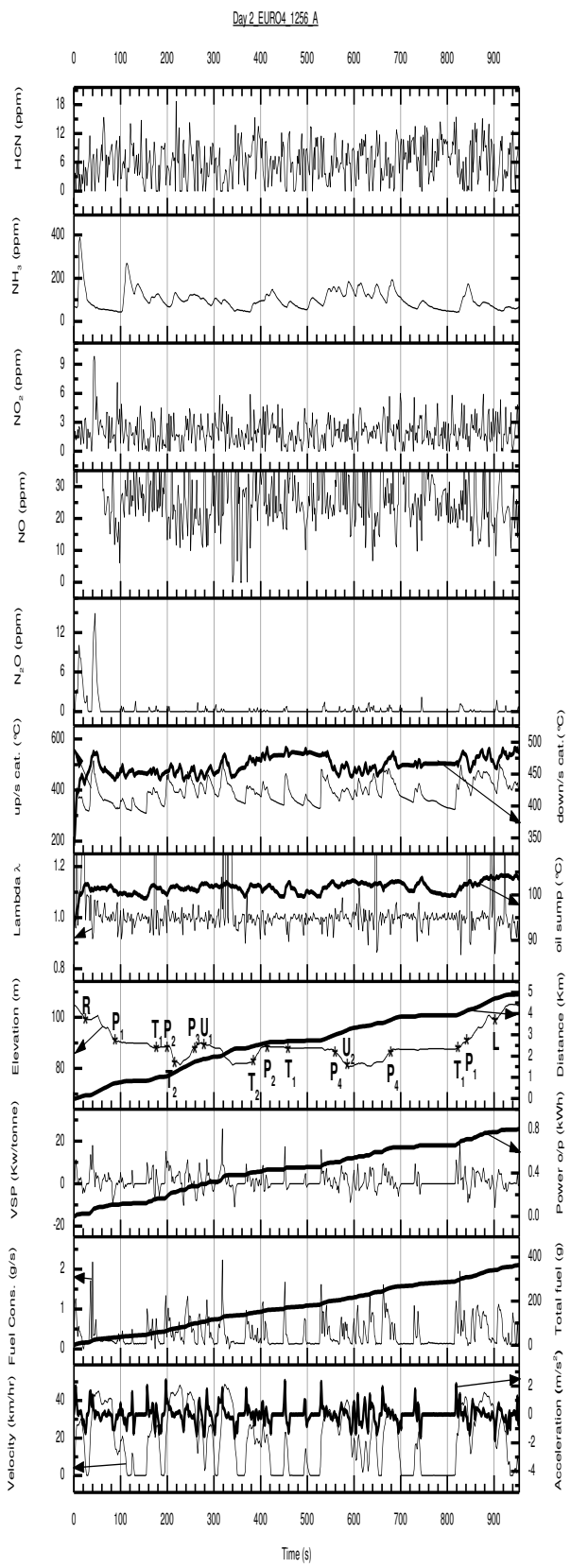

Figure 6: Profiles for the trip 12:56A-a

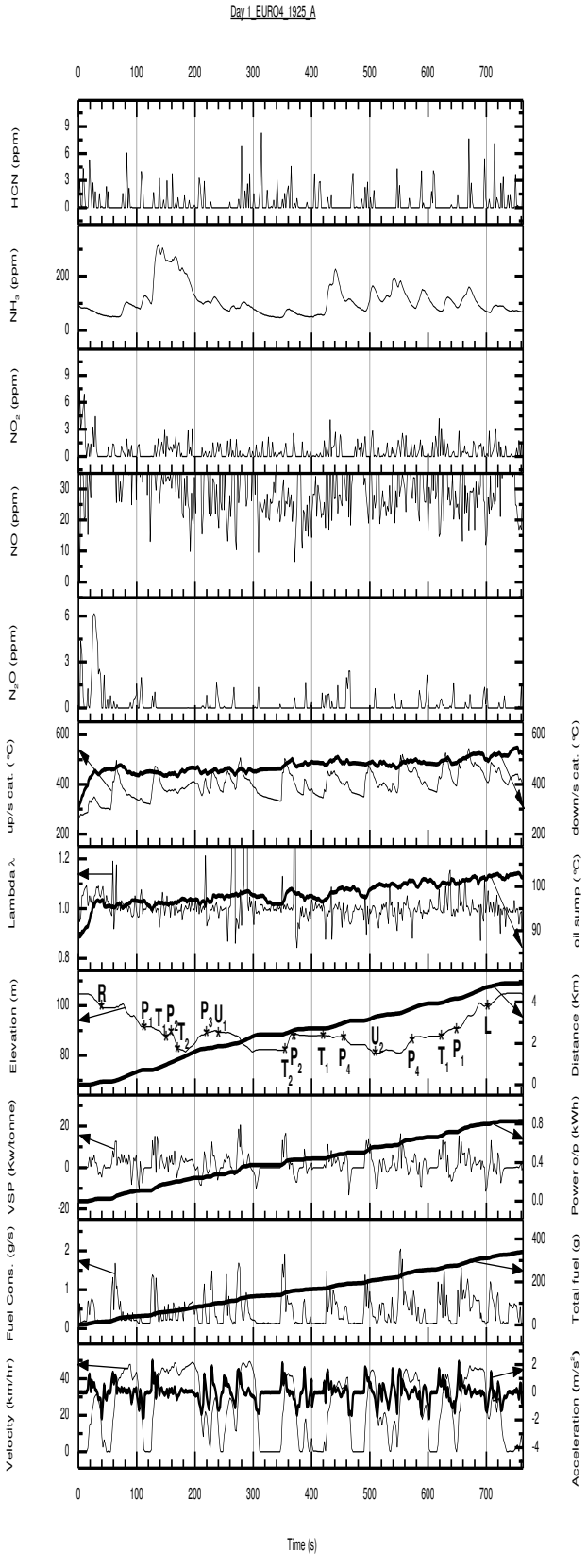

Figure 7: Profiles for the trip 19:25A-a

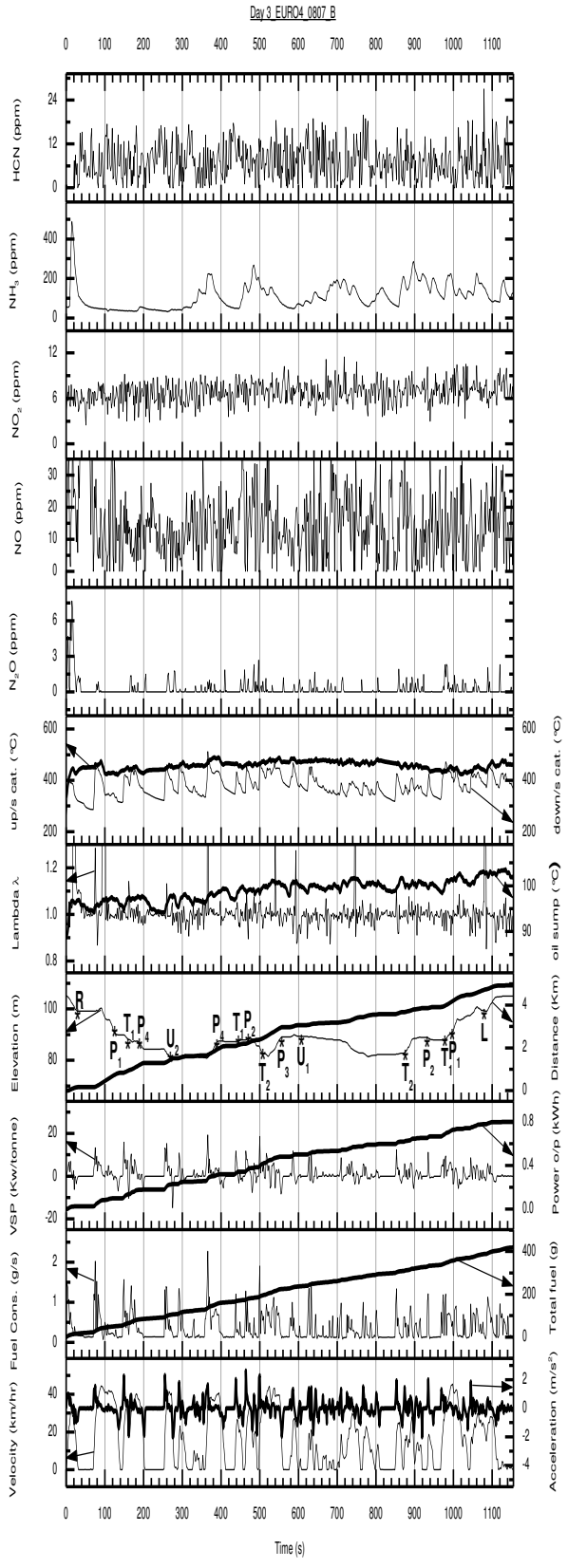

Figure 8: Profiles for the trip 8:07B-a

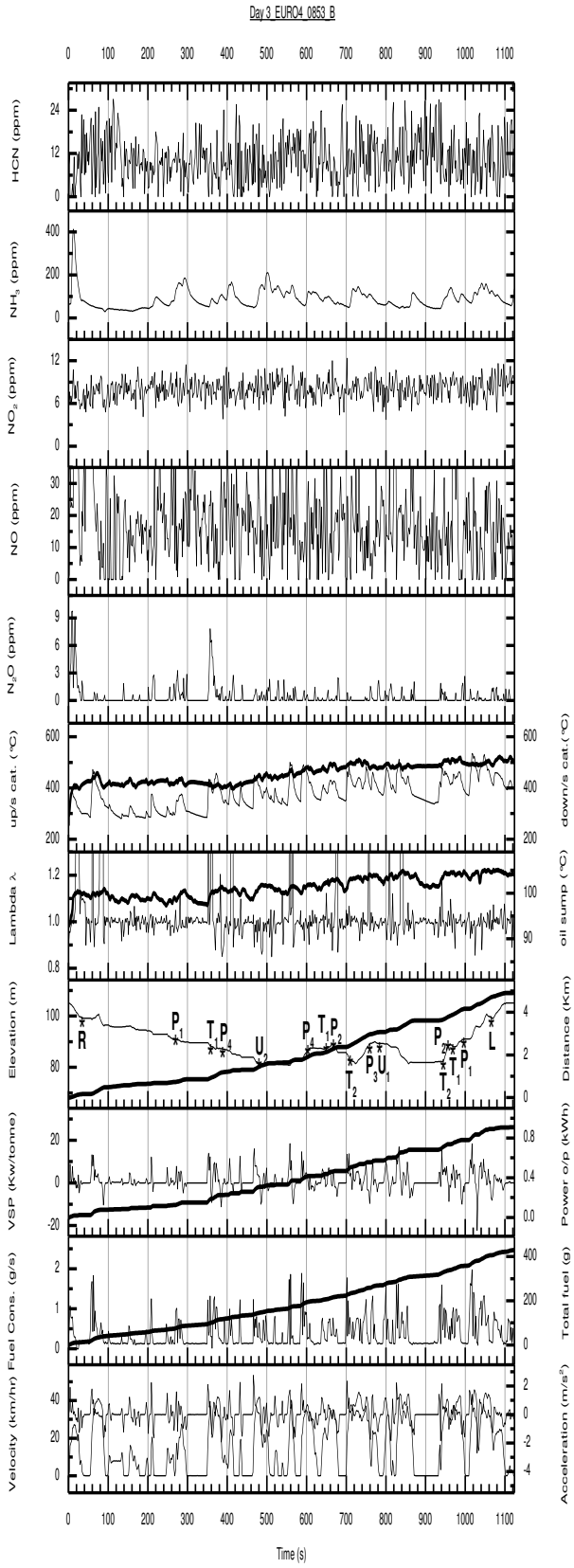

Figure 9: Profiles for the trip 8:53B-a

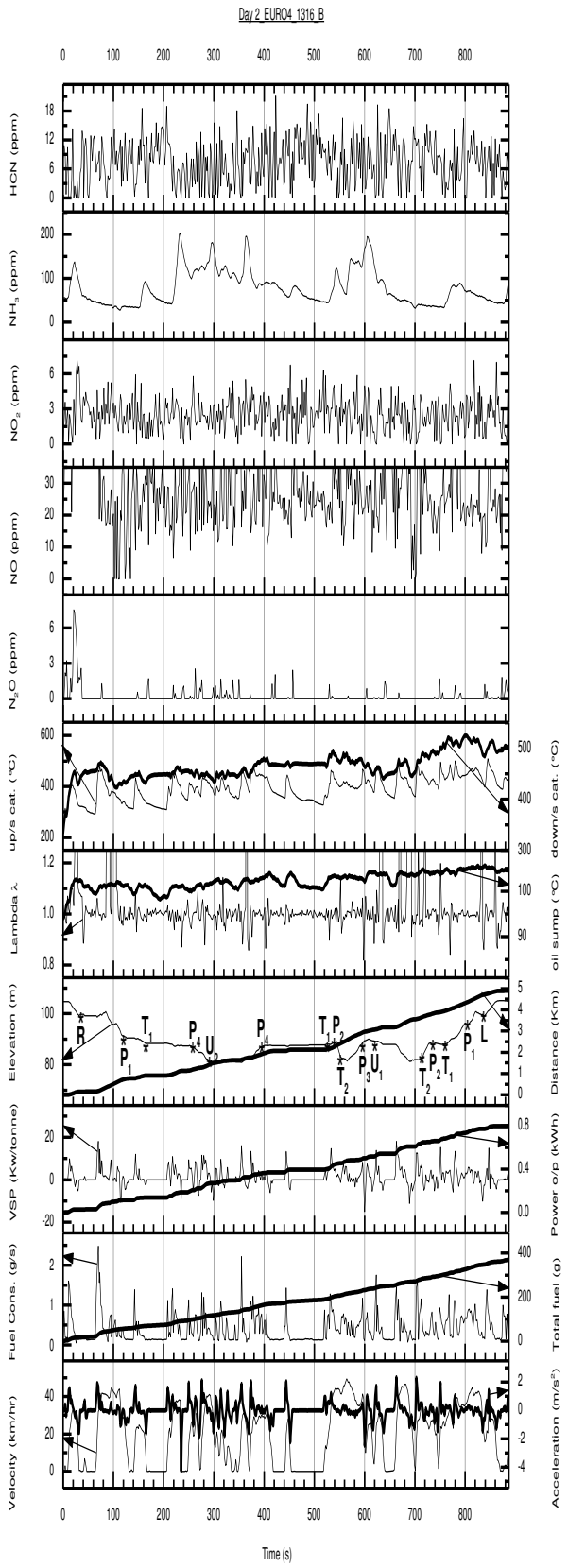

Figure 10: Profiles for the trip 13:16B-a

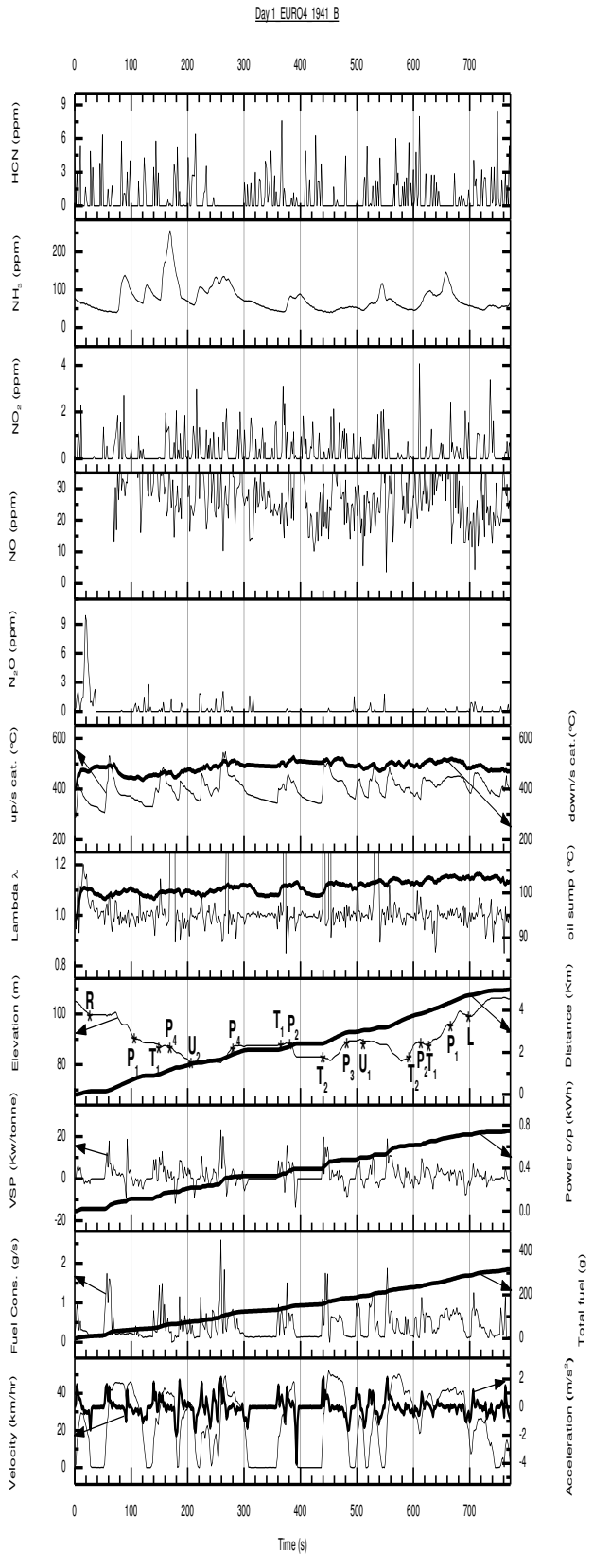

Figure 11: Profiles for the trip 19:41B-a

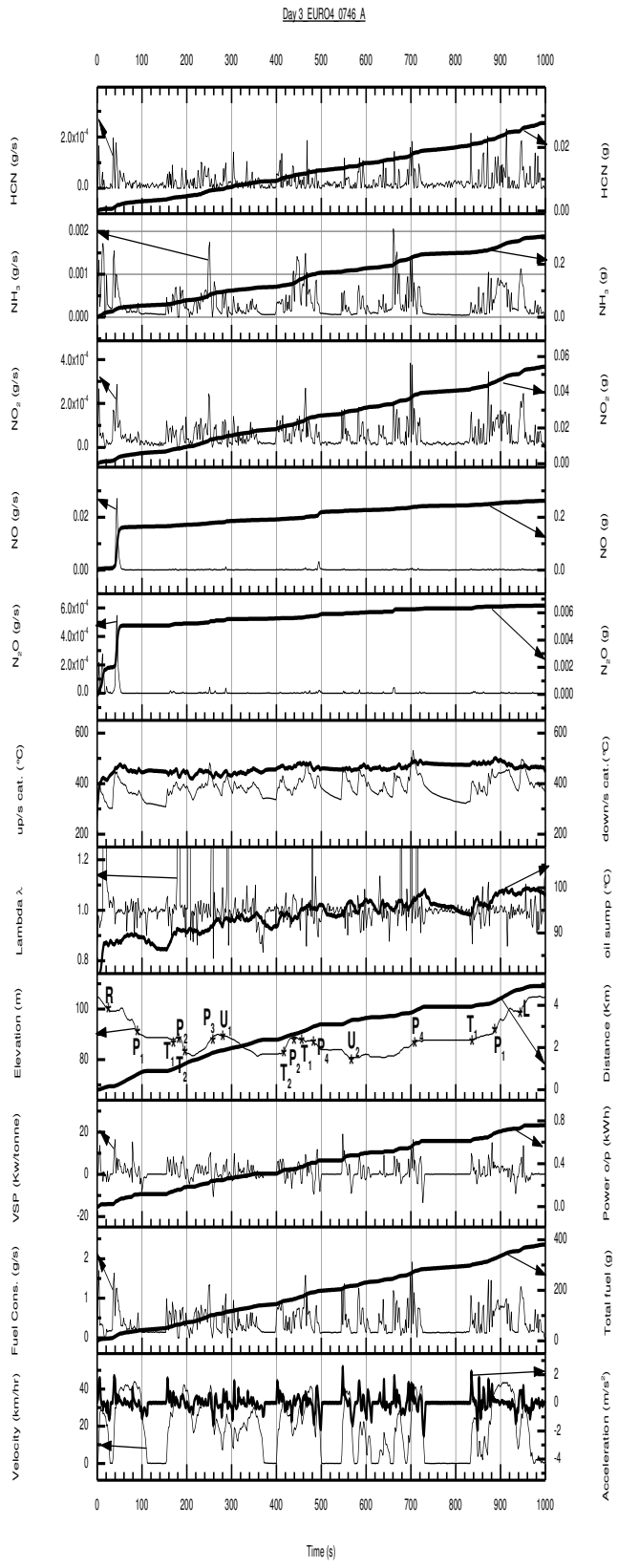

Figure 12: Profiles for the trip 7:46A-b

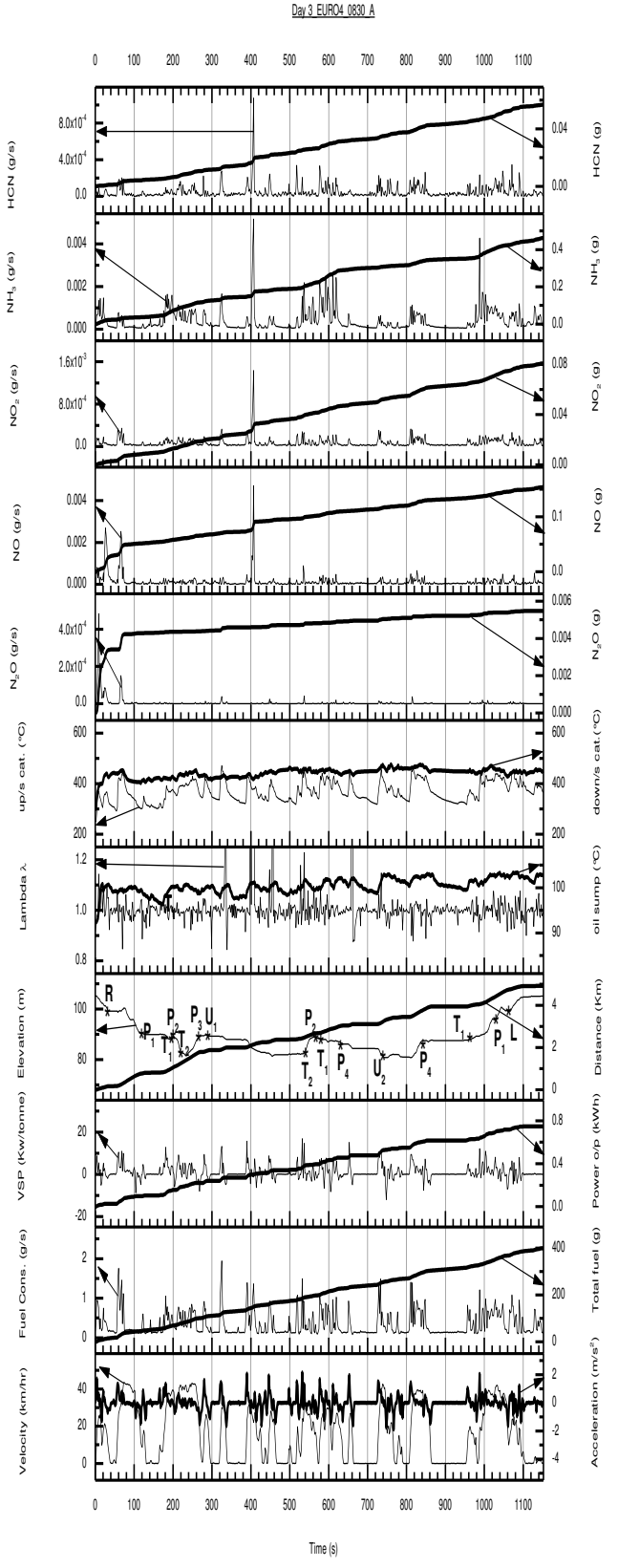

Figure 13 Profiles for the trip 8:30A-b

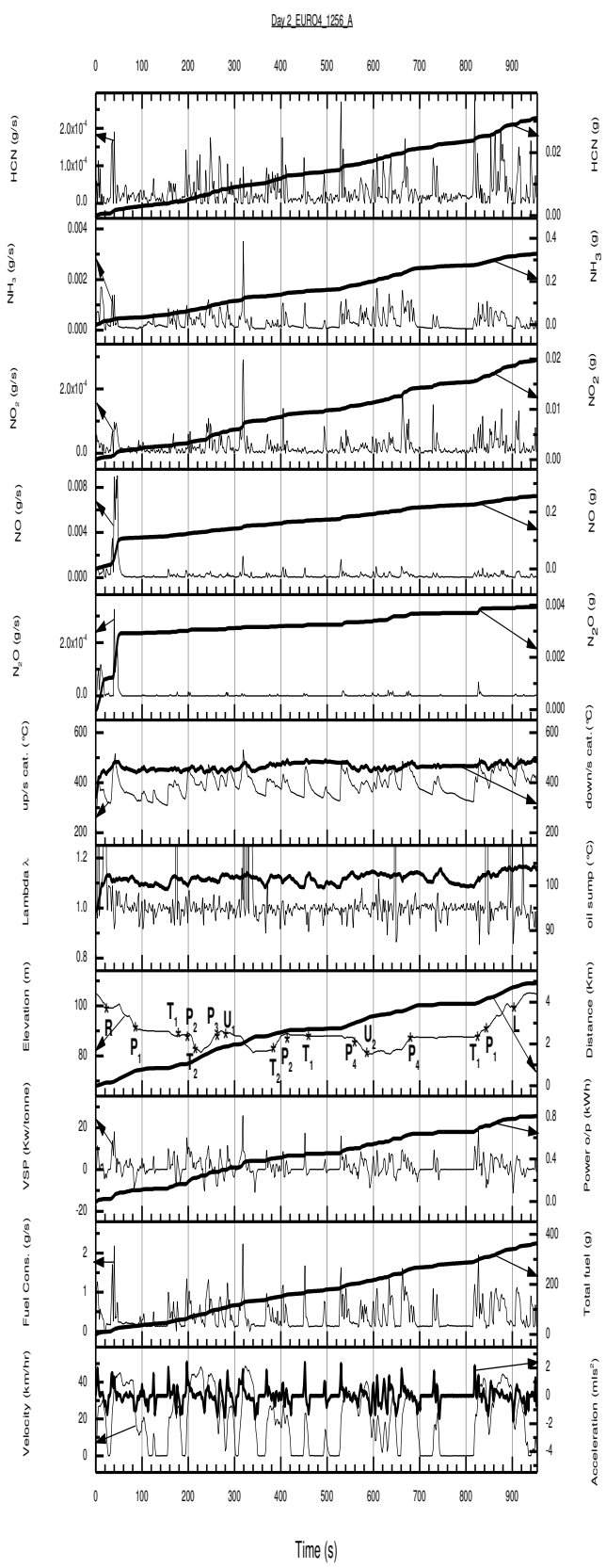

Figure 14: Profiles for the trip 12:56A-b

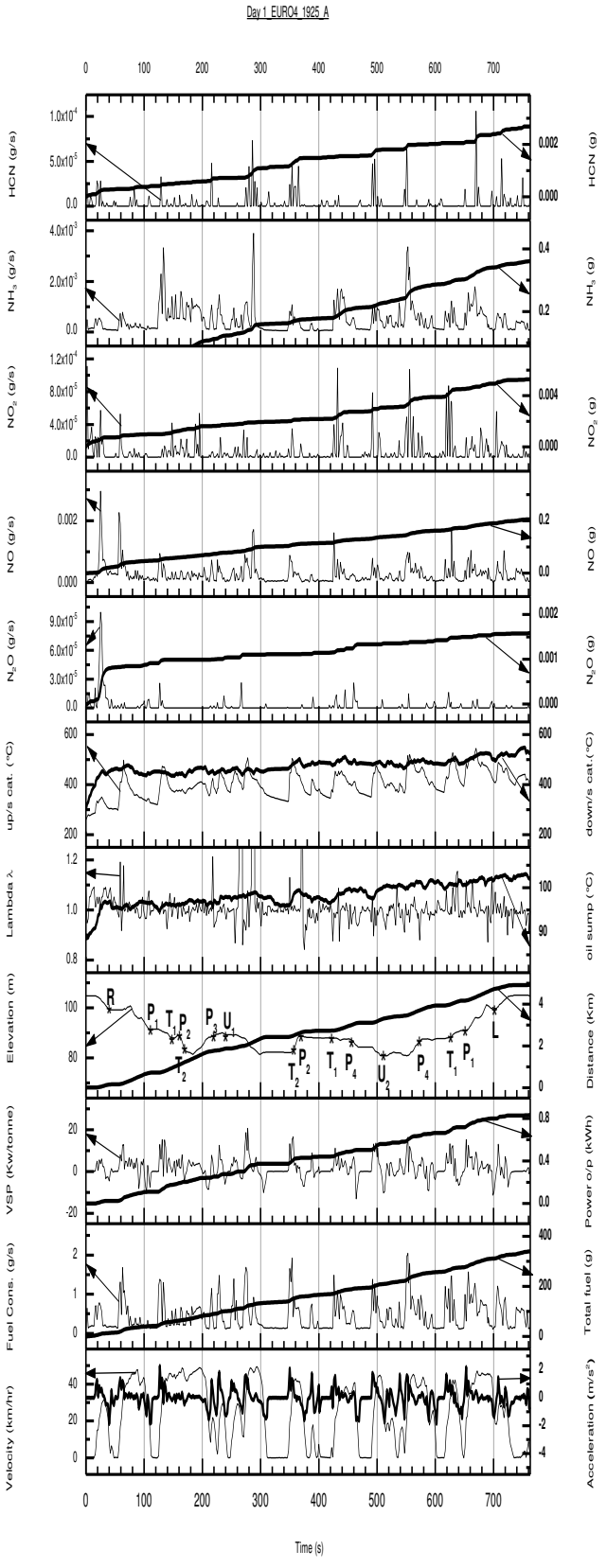

Figure 15: Profiles for the trip 19:25A-b

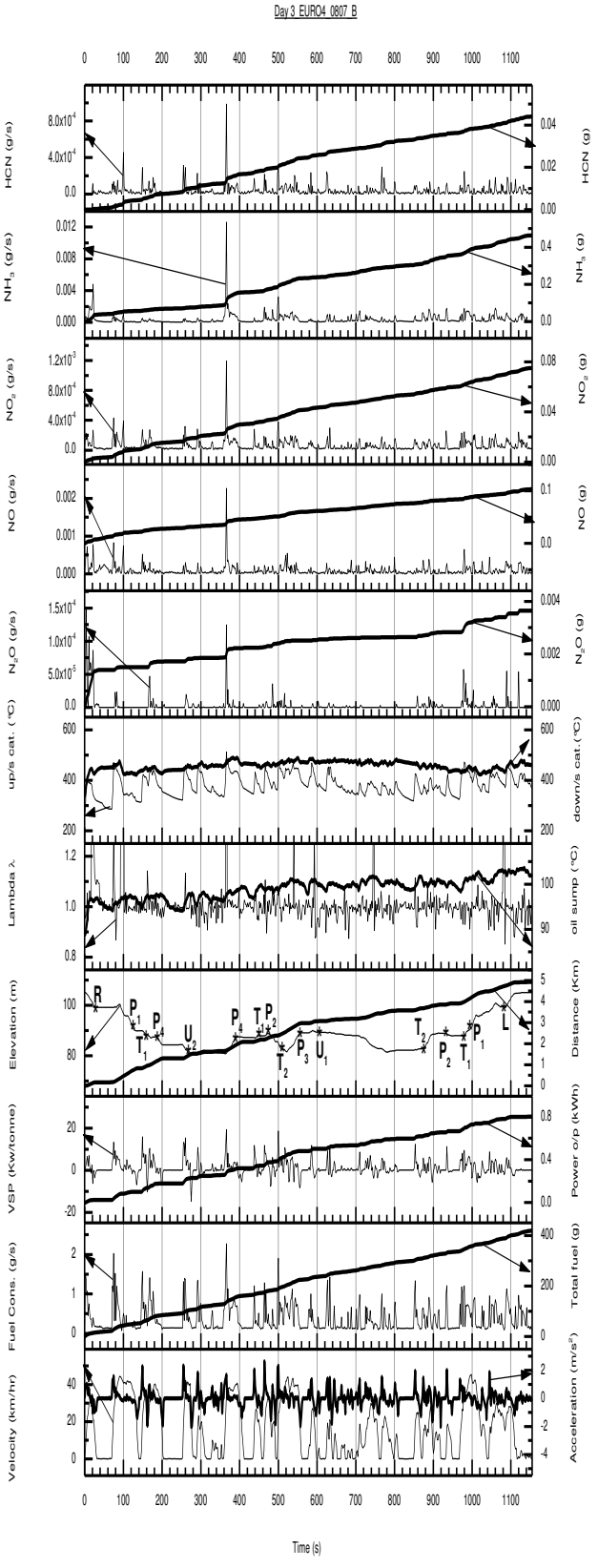

Figure 16: Profiles for the trip 8:07B-b

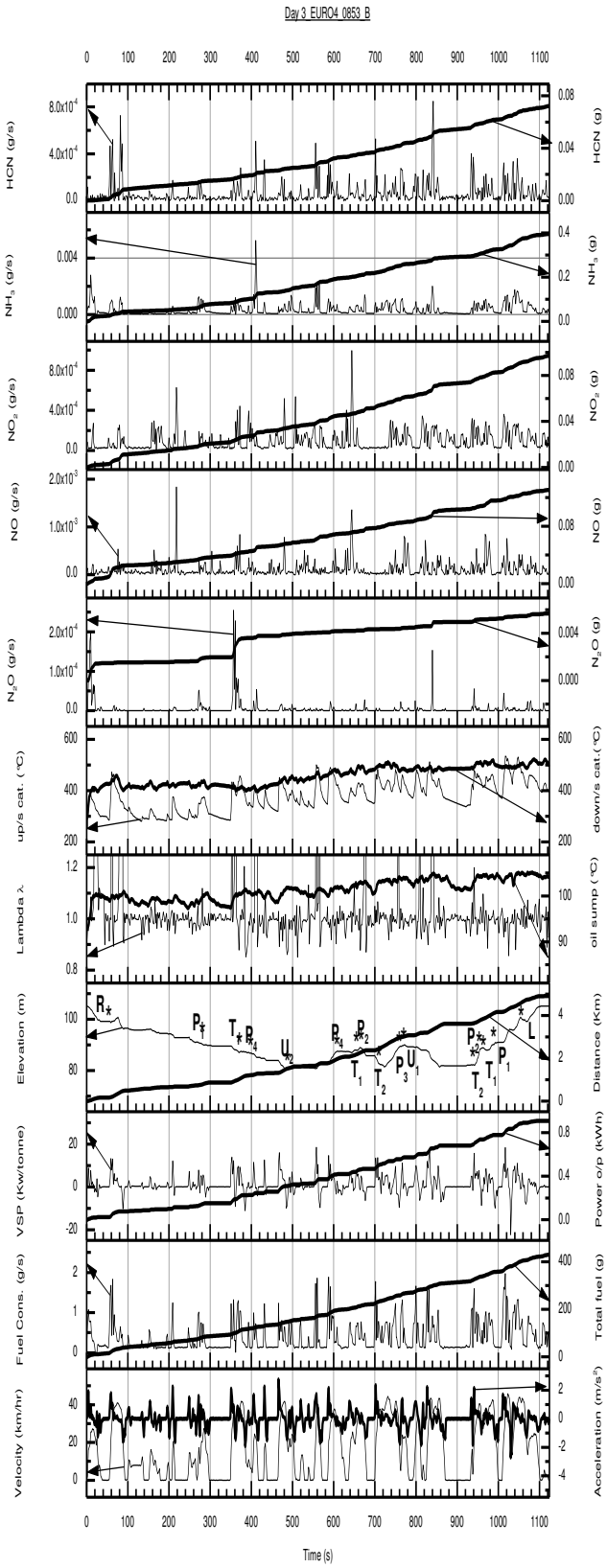

Figure 17: Profiles for the trip 8:53B-b

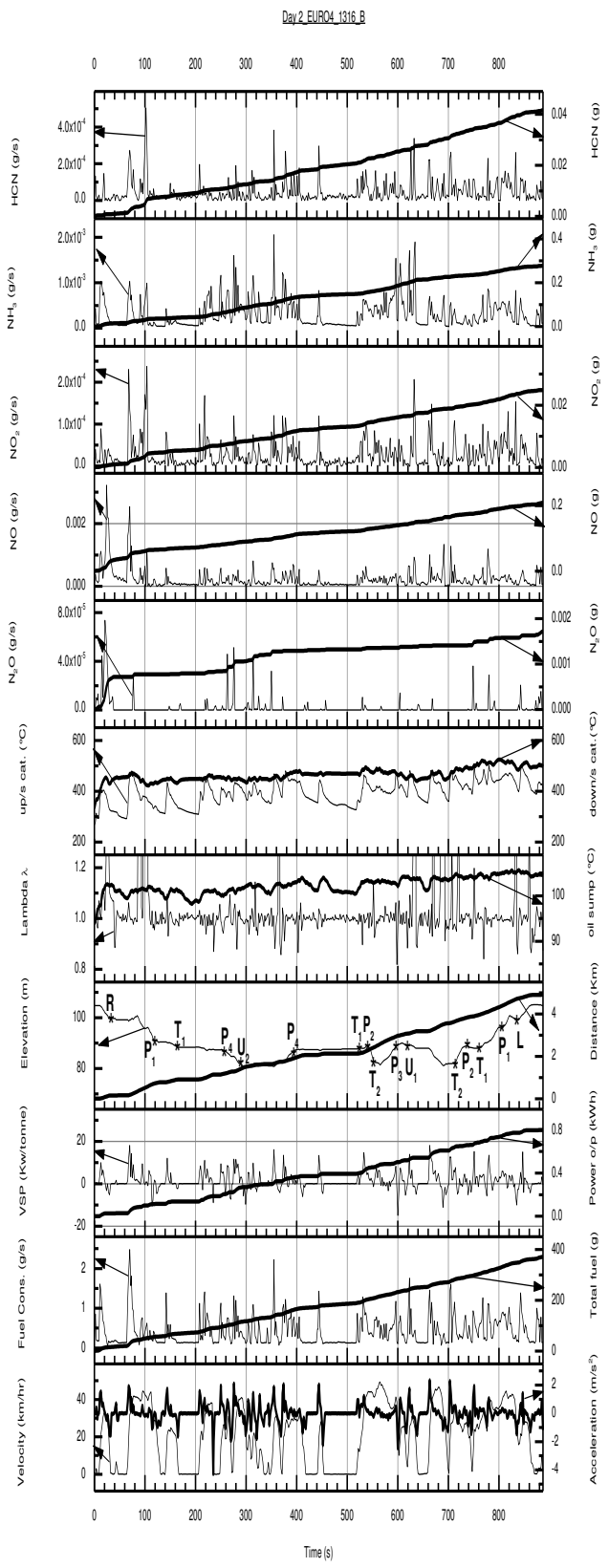

Figure 18: Profiles for the trip 13:16B-b

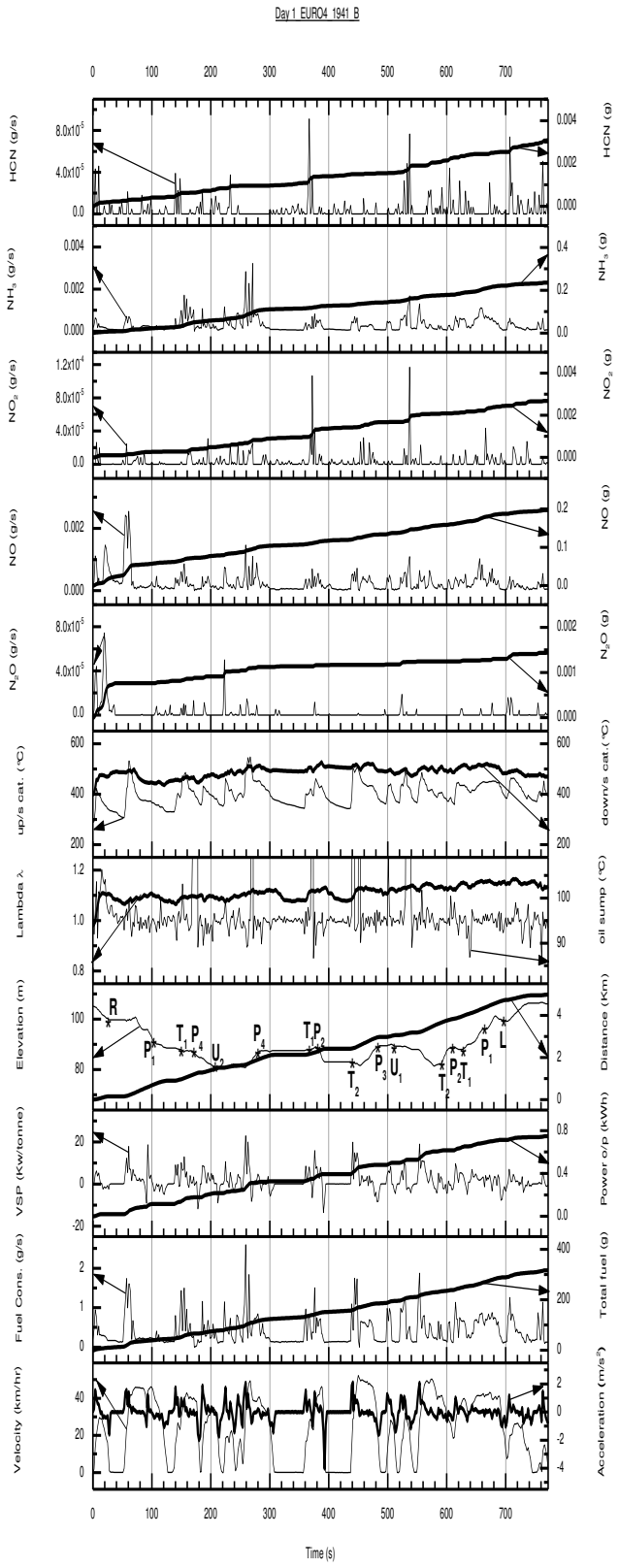

Figure 19: Profiles for the trip 19:41B-b

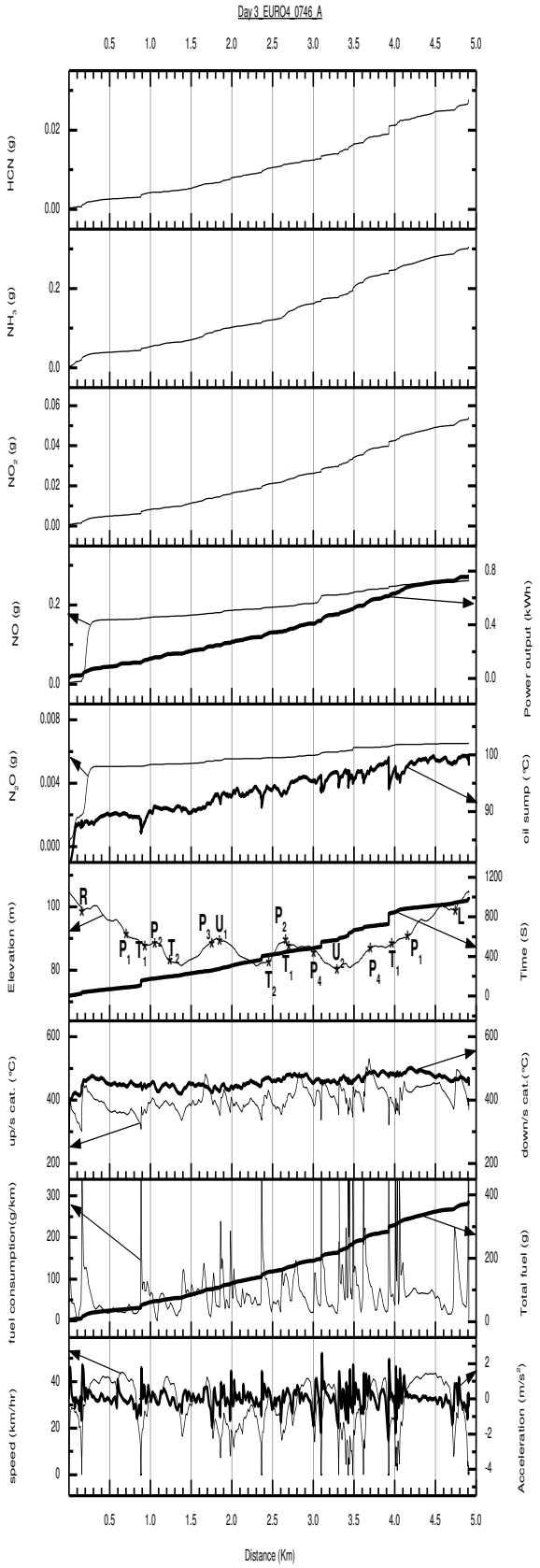

Figure 20: Profiles for the trip 7:46A-c

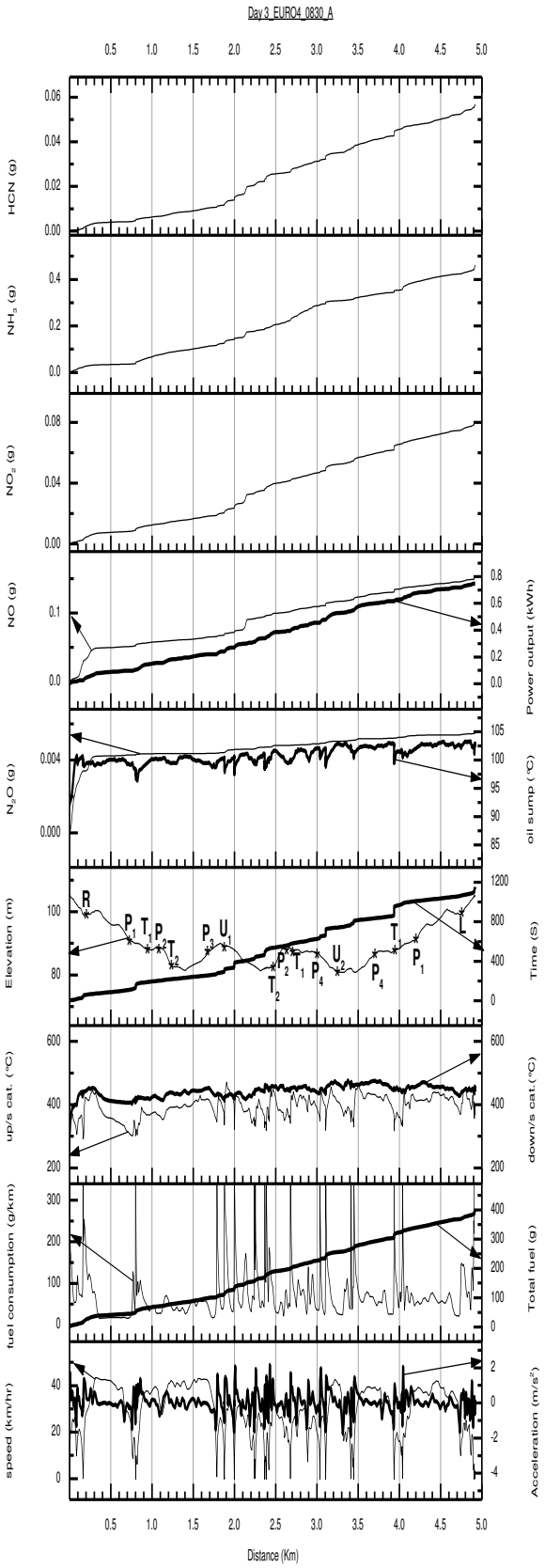

Figure 21: Profiles for the trip 8:30A-c

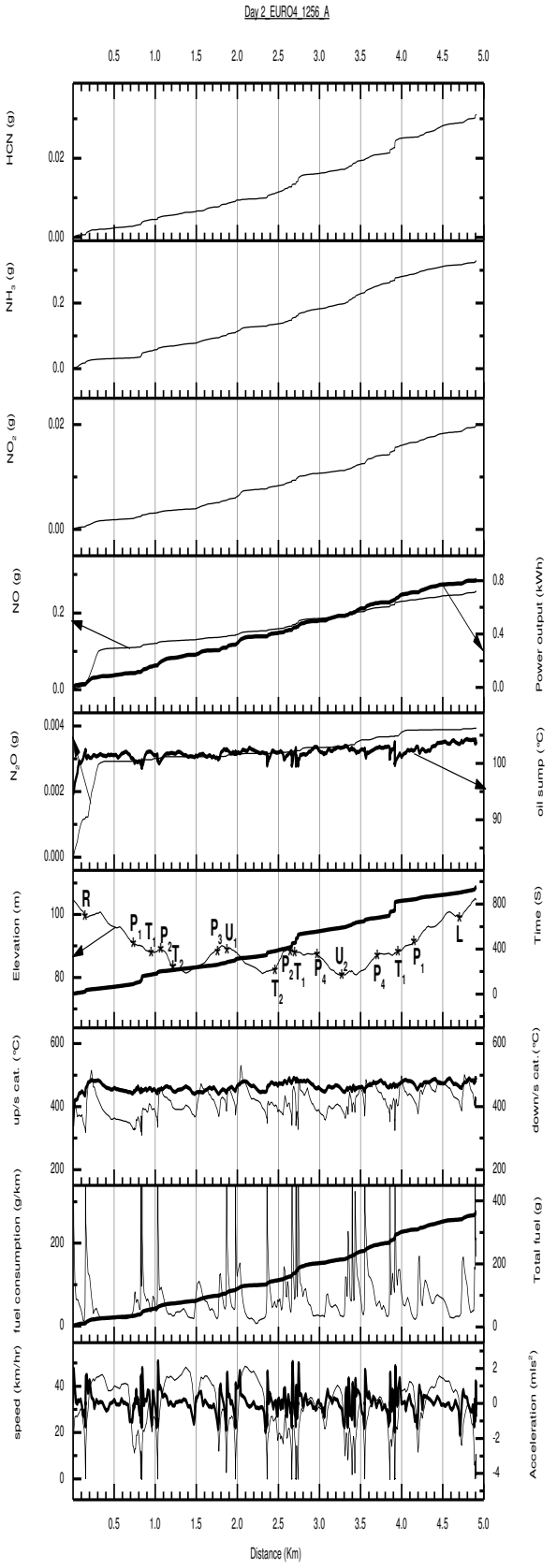

Figure 22: Profiles for the trip 12:56A-c

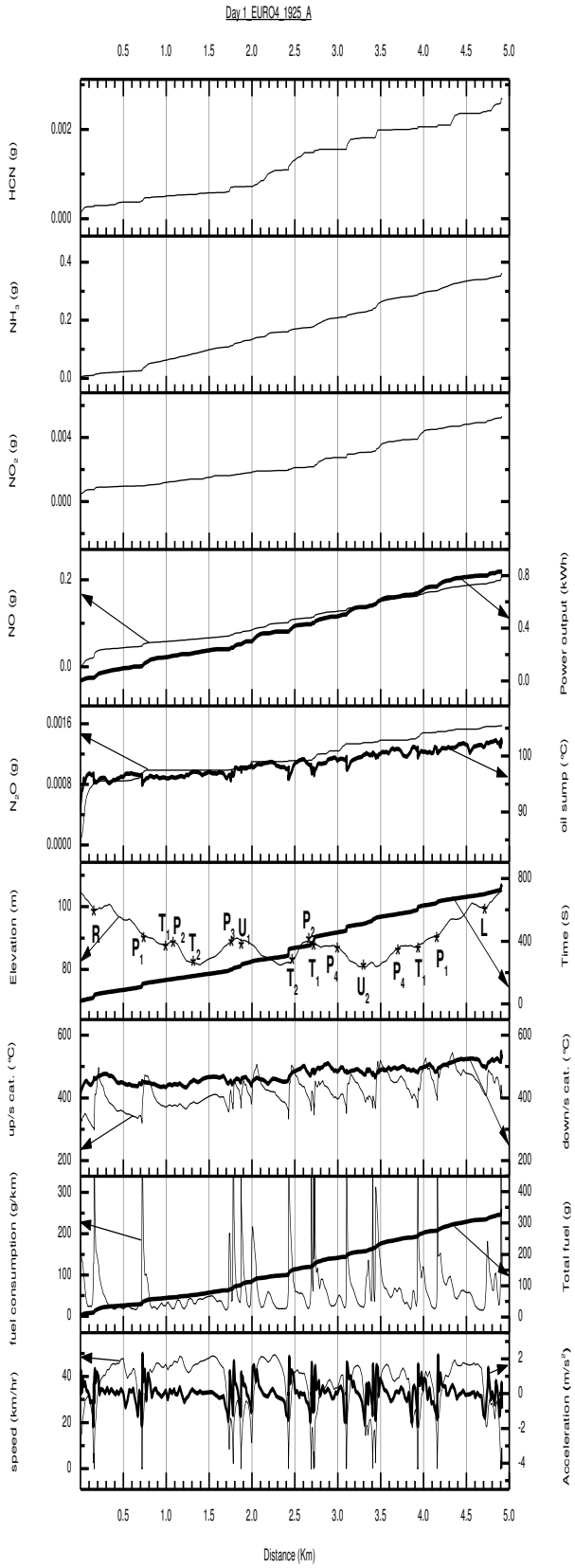

Figure 23: Profiles for the trip 19:25A-c

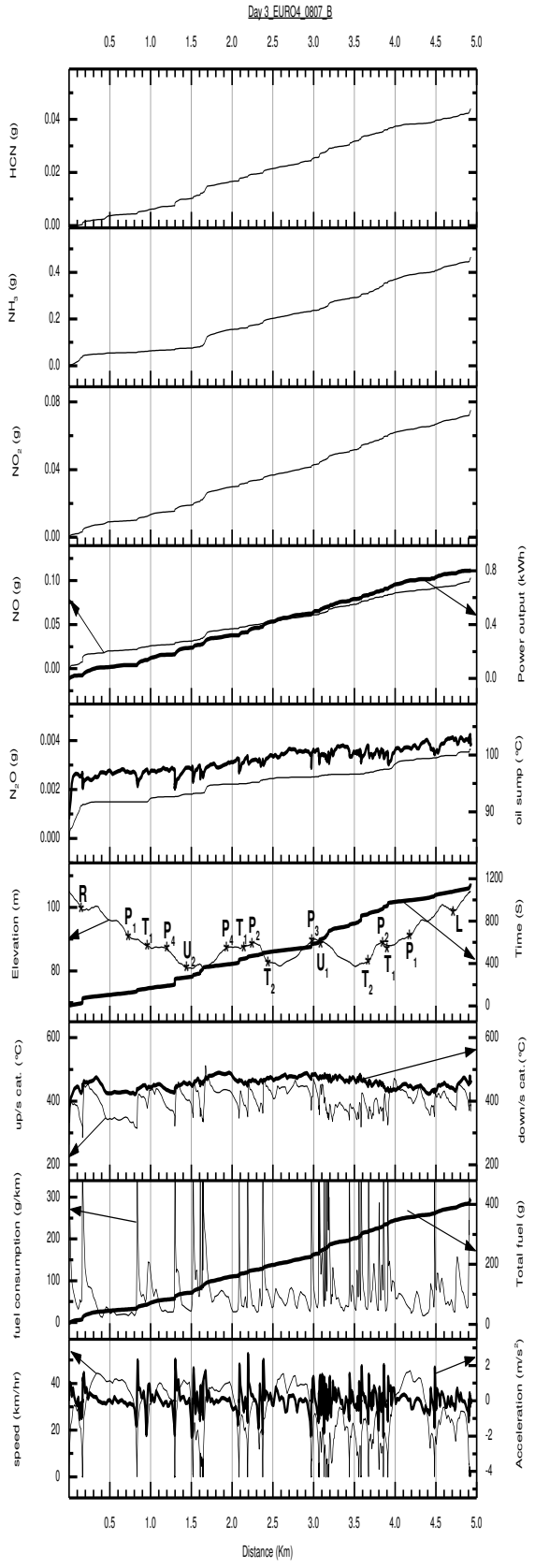

Figure 24: Profiles for the trip 8:07B-c

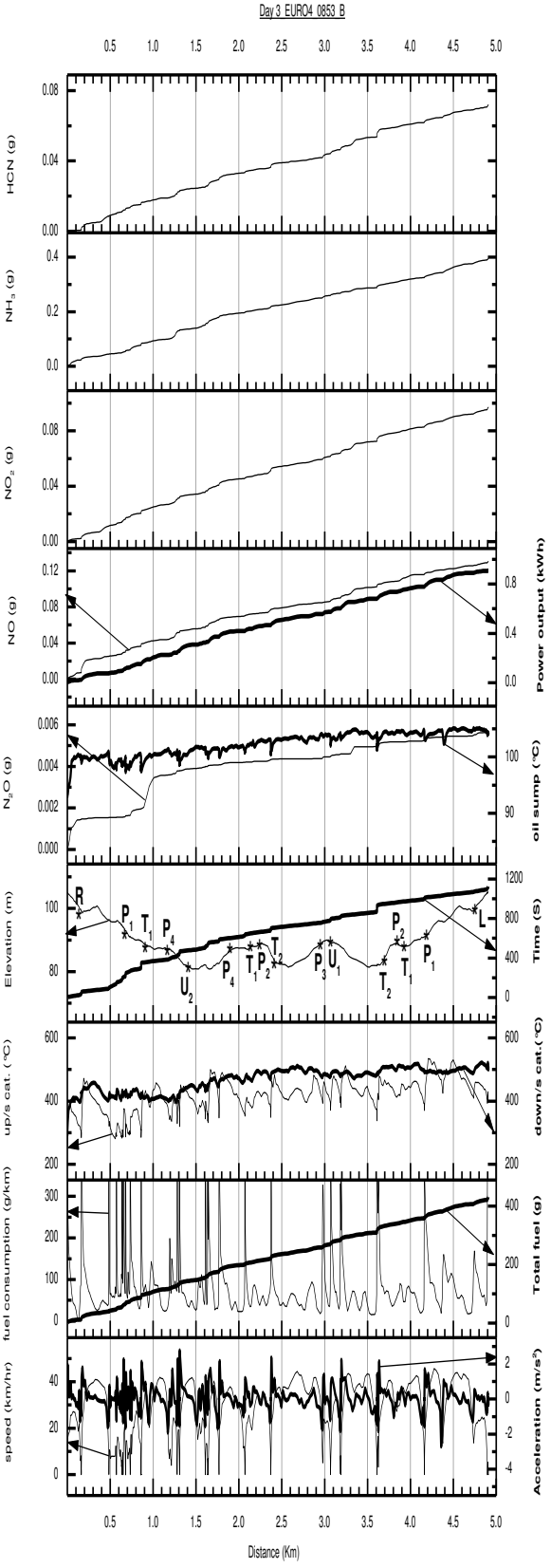

Figure 25: Profiles for the trip 8:53B-c

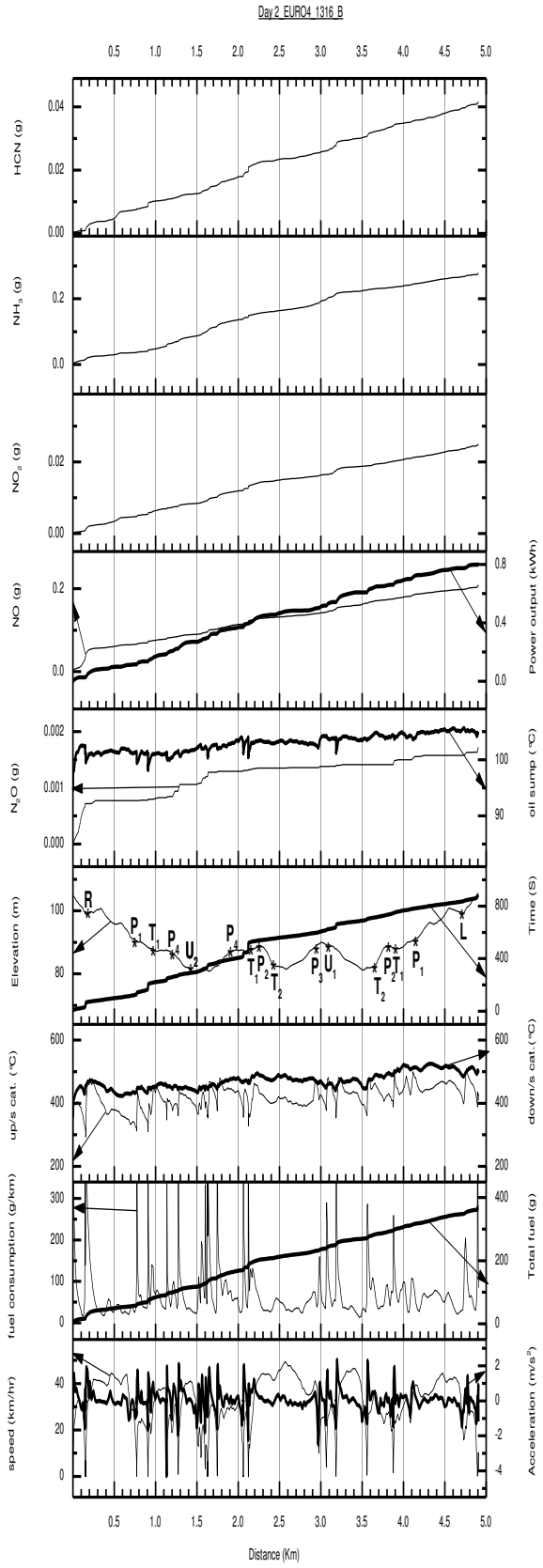

Figure 26: Profiles for the trip 13:16B-c

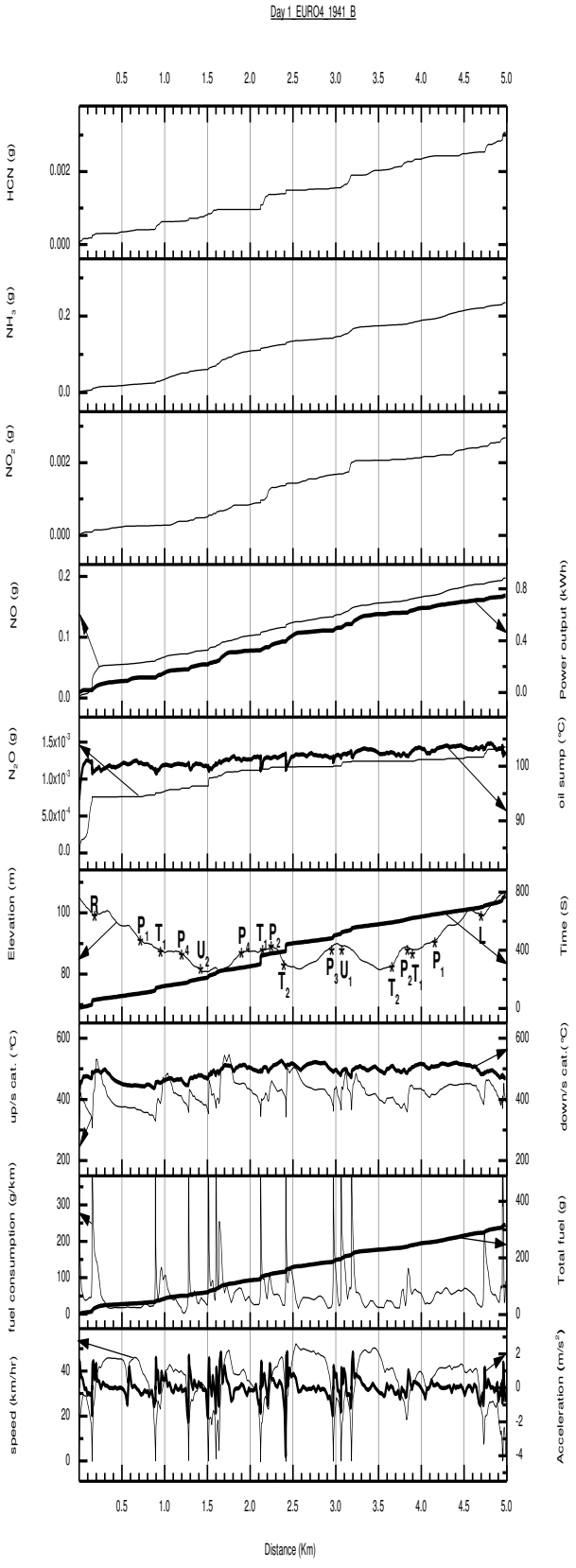

Figure 27: Profiles for the trip 19:41B-c

Correlations between emissions and driving parameters

Figures 28 to 32 present the relationship between emissions of five nitrogen compounds and trip average velocity for eight trips. NO2 and HCN showed good linear negative correlation with trip average velocity. Increasing the average velocity will decrease the emissions of NO_2 and HCN. NH3 and N2O showed a moderate negative correlation with the average velocity. There was no correlation observed for NO with the average velocity.

Figures 33 to 37 present the relationship between emissions of five nitrogen compounds and trip average acceleration for eight trips. There were no correlations observed between all five nitrogen compounds and average accelerations.

Figure 38 to 42 present the relationship between emissions of five nitrogen compounds and trip average VSP for eight trips. NO2 and N2O showed good negative linear correlation with average VSP. NH3 and HCN showed a moderate negative correlation with average VSP. There was no correlation observed between NO and average VSP.

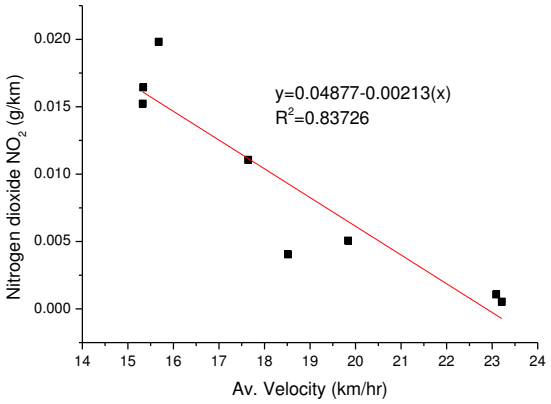

Figure 28: Trip mean NO_2 emissions Vs vehicle's average trip velocity

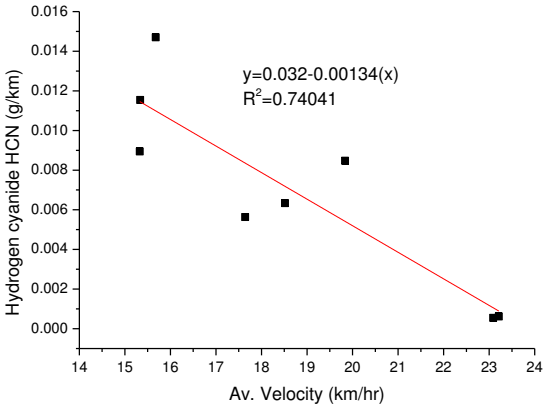

Figure 29: Trip mean HCN emissions Vs vehicle's average trip velocity

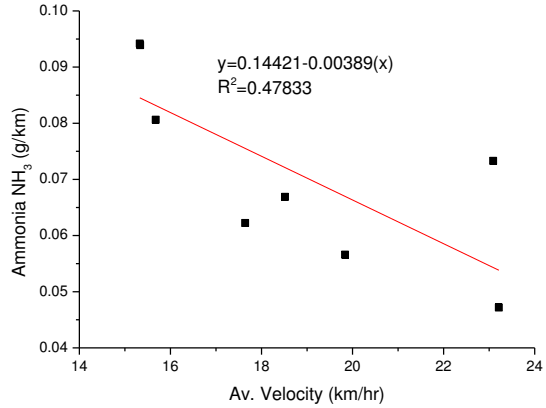

Figure 30: Trip mean NH_3 emissions Vs vehicle's average trip velocity

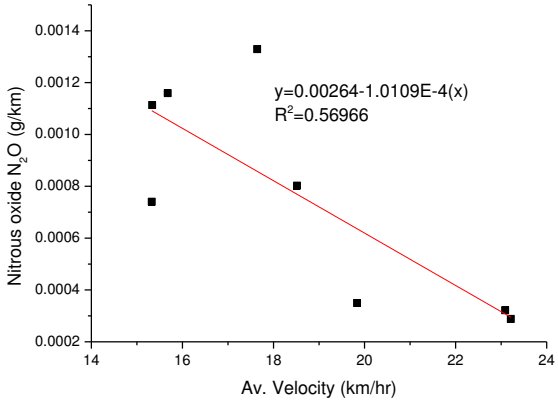

Figure 31: Trip mean N_2O emissions Vs vehicle's average trip velocity

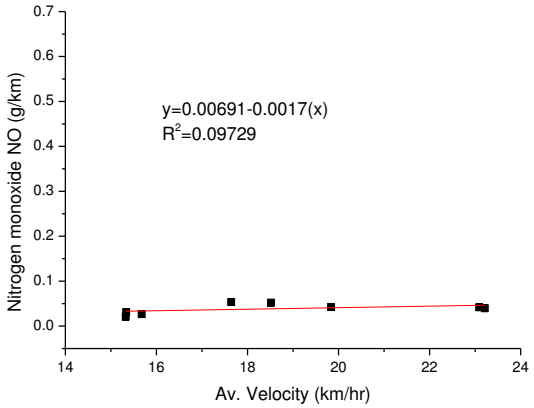

Figure 32: Trip mean NO emissions Vs vehicle's average trip velocity

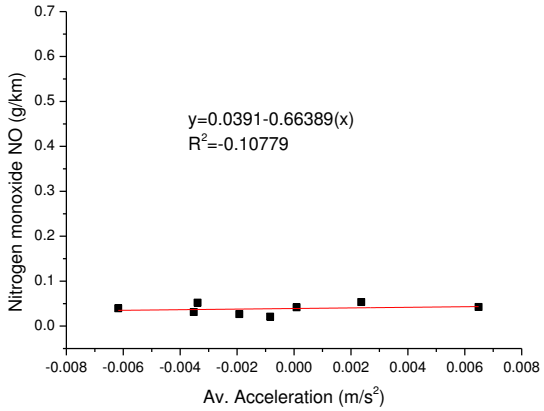

Figure 35: Trip mean NO emissions Vs vehicle's average trip acceleration

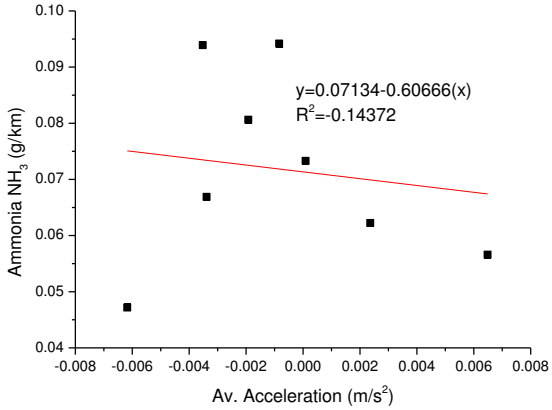

Figure 33: Trip mean NH_3 emissions Vs vehicle's average trip acceleration

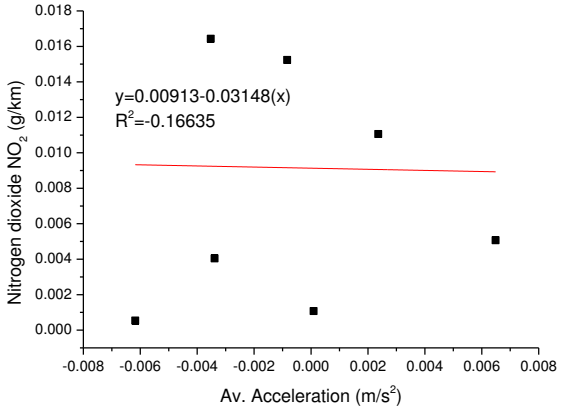

Figure 36: Trip mean NO_2 emissions Vs vehicle's average trip acceleration

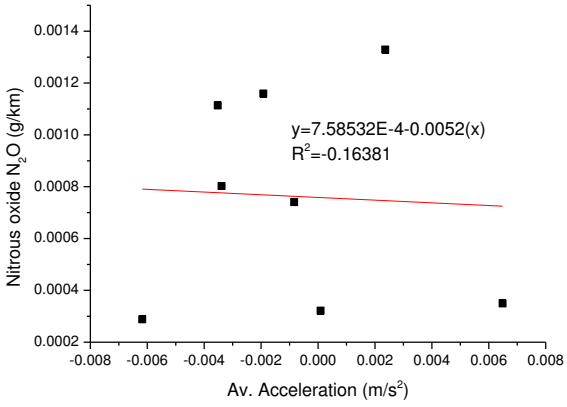

Figure 34: Trip mean N_2O emissions Vs vehicle's average trip acceleration

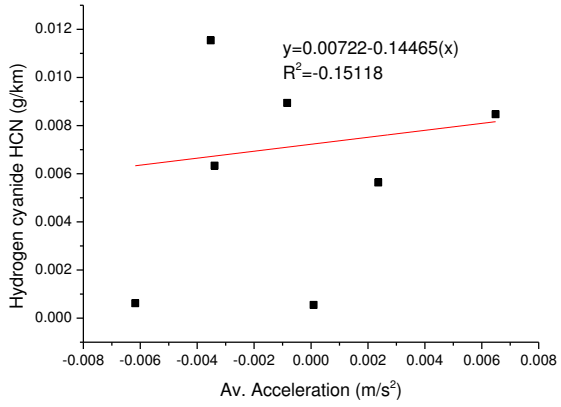

Figure 37: Trip mean HCN emissions Vs vehicle's average trip acceleration

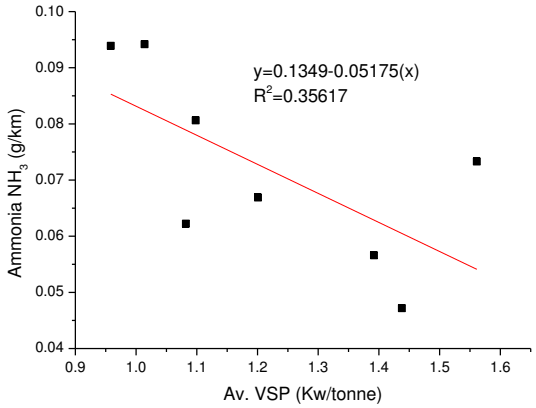

Figure 38: Trip mean NH_3 emissions Vs vehicle's average trip vehicle specific power

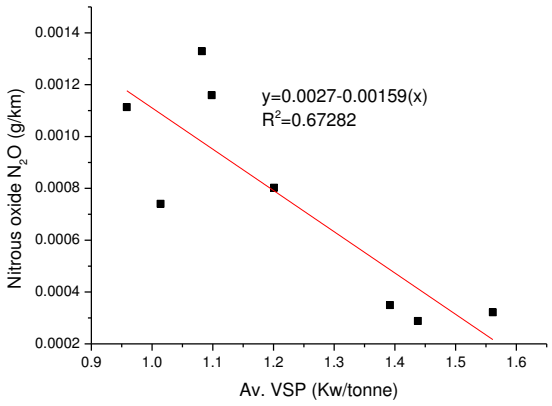

Figure 39: Trip mean N_2O emissions Vs vehicle's average trip vehicle specific power

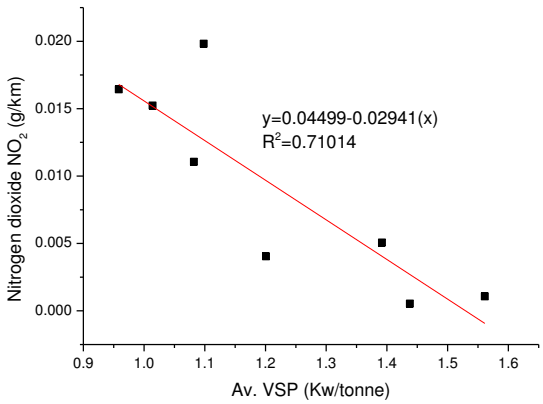

Figure 40: Trip mean NO_2 emissions Vs vehicle's average trip vehicle specific power

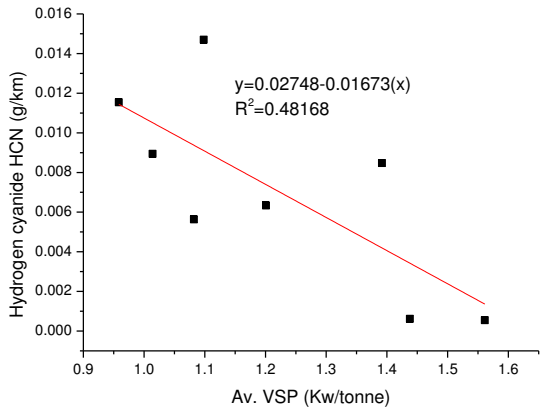

Figure 41: Trip mean HCN emissions Vs vehicle's average trip vehicle specific power

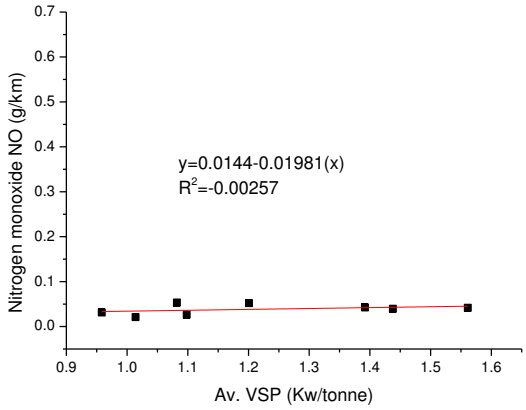

Figure 42: Trip mean NO emissions Vs vehicle's average trip vehicle specific power

Conclusions

Nitrogen compound emissions (HCN, NO, NO2, N2O and NH3) from a EURO4 SI passenger car were measured using a portable FTIR system. The vehicle was driven on two real world driving cycles (route A and B) using the routes located in a dense populated area of Leeds representing typical urban road network. Eight real world emission tests were conducted at different times of days such as the morning rush hours, lunch time and off-peak time in the evening. The emissions were presented in ppm, g/s and g/km. The correlations between five nitrogen compounds emissions and trip average velocity, acceleration and VSP were analyzed. The results have shown that:

1. NO2 and NH3 emissions are the most abundant nitrogen species in the tailpipe and can be detected from all the trips. NO2 and HCN can be detected from 6 relatively congested trips but not from two evening free flow trips. This reflected that frequent stop and start and associated accelerations can increase nitrogen compound emissions.
2. NH3 emissions from this research were significantly higher than some reported data from other Euro 4 SI cars using NEDC. One of the major reasons for this is due to the real driving cycles used in this research had more frequent stop and start and more harsh accelerations.
3. The results of mass emissions as a function of distance travelled showed clear evidences of the accumulation of emissions during vehicle's stoppage periods at traffic lights and in the queues.
4. NO2 and HCN showed good linear negative correlations with trip average velocity. NH3 and N2O showed a moderate negative correlation with the average velocity. There was no correlation observed for NO with the average velocity.
5. There were no correlations observed between all five nitrogen compounds and average accelerations.
6. NO2 and N2O showed good negative linear correlations with average VSP. NH3 and HCN showed a moderate negative correlation with average VSP. There was no correlation observed between NO and average VSP.

Contact Information

Dr. Hu Li, Energy Research Institute, School of Process, Environmental and Materials Engineering, the University of Leeds. Email: fuehli@leeds.ac.uk.

Acknowledgments

Ahmad Khalfan would like to thank Kuwait government for a PhD scholarship to support his study at Leeds University. Data used in this paper were collected during a EPSRC funded project RETEMM (Real-world Traffic Emissions Measurement and Modeling) and thus thanks go to EPSRC and RETEMM team, specifically for Dr. James Tate and Dr. Karl Ropkins who were part of the team.

Definitions/Abbreviations

FTIR: Fourier Transform Infrared sample abbreviations

NEDC: New European Driving Cycle

VSP: Vehicle Specific Power

References

1. Hawirko, J.D. and M.D. Checkel, *Quantifying Vehicle Emission Factors for Various Ambient Conditions using an On-Road, Real-Time Emissions System*, 2003, SAE International.DOI: 10.4271/2003-01-0301.
2. Li, H., et al., *Impact of Driving Cycles on Greenhouse Gas (GHG) Emissions, Global Warming Potential (GWP) and Fuel Economy for SI Car Real World Driving.* SAE International Journal of Fuels and Lubricants 2009. **Volume 1 (1):**: p. 1320-1333.DOI: 10.4271/2008-01-1749
3. Li, H., et al., *Characterization of Regulated and Unregulated Cold Start Emissions for Different Real World Urban Driving Cycles Using a SI Passenger Car. SAE Technical Paper Series 2008-01-1648*, 2008, SAE International.DOI: 10.4271/2008-01-1648.
4. Li, H., et al., *Analysis of Driving Parameters and Emissions for Real World Urban Driving Cycles using an on-board Measurement Method for a EURO 2 SI car. SAE Technical Paper Series 2007-01-2066/JSAE 20077353*, in *The JSAE International Fuels and Lubes Conference* 2007, SAE International/JSAE: Kyoto, Japan.DOI: 10.4271/2007-01-2066.
5. Li, H., et al., *Impact of Traffic Conditions and Road Geometry on Real world Urban Emissions Using a SI Car. SAE Technical Paper Series 2007-01-0308*, in *Emissions measurement and testing, 2007 (SP-2089)*2007, SAE International.
6. Li, H., et al., *Study of the Emissions Generated at Intersections for a SI Car under Real World Urban Driving Conditions*, 2006, SAE International.DOI: 10.4271/2006-01-1080.
7. Tziraks, E., K. Pitsas, F. Zannikos, and S. Stournas, *Vehicle Emissions and Drivng Cycles: Comparison of the Athens Driving Cycle (ADC) with ECE-15 and European Driving Cycle (EDC).* Global Nest, 2006. **8**(3): p. 282-290
8. Wang, A., et al., *On-road pollutant emission and fuel consumption characteristics of buses in Beijing.* Journal of Environmental Sciences, 2011. **23**(3): p. 419-426.DOI: http://dx.doi.org/10.1016/S1001-0742(10)60426-3

9. Wang, X.M., G. Carmichael, D.L. Chen, Y.H. Tang, and T.J. Wang, *Impacts of different emission sources on air quality during March 2001 in the Pearl River Delta (PRD) region.* Atmospheric Environment, 2005. **39**(29): p. 5227-5241
10. Wyatt, D.W., H. Li, and J. Tate, *Examining the Influence of Road Grade on Vehicle Specific Power (VSP) and Carbon Dioxide (CO2) Emission over a Real-World Driving Cycle*, 2013, SAE International.DOI: 10.4271/2013-01-1518.
11. Finlayson-Pitts, B.J. and J.N. Pitts, Jr., *Tropospheric air pollution: ozone, airborne toxics, polycyclic aromatic hydrocarbons, and particles.* Science, 1997. **276**(5315): p. 1045-52
12. UN. *Guidance documents and other methodological materials for the implementation of the 1999 Protocol to Abate Acidification, Eutrophication and Ground-level Ozone (Gothenburg Protocol)* United Nations Economic Commission for Europe 1999.
13. Heeb, N.V., et al., *Three-way catalyst-induced formation of ammonia—velocity- and acceleration-dependent emission factors.* Atmospheric Environment, 2006. **40**(31): p. 5986-5997.DOI: http://dx.doi.org/10.1016/j.atmosenv.2005.12.035
14. Heeb, N.V., C.J. Saxer, A.-M. Forss, and S. Brühlmann, *Correlation of hydrogen, ammonia and nitrogen monoxide (nitric oxide) emissions of gasoline-fueled Euro-3 passenger cars at transient driving.* Atmospheric Environment, 2006. **40**(20): p. 3750-3763.DOI: http://dx.doi.org/10.1016/j.atmosenv.2006.03.002
15. Heeb, N.V., C.J. Saxer, A.-M. Forss, and S. Brühlmann, *Trends of NO-, NO2-, and NH3-emissions from gasoline-fueled Euro-3- to Euro-4-passenger cars.* Atmospheric Environment, 2008. **42**(10): p. 2543-2554.DOI: http://dx.doi.org/10.1016/j.atmosenv.2007.12.008
16. Liu, I.Y. and N. Cant, *The Formation and Reactions of Hydrogen Cyanide During Isobutane-SCR over Fe-MFI Catalysts.* Catalysis Surveys from Asia, 2003. **7**(4): p. 191-202.DOI: 10.1023/B:CATS.0000008160.18010.cb
17. Karlsson, H.L., *Ammonia, nitrous oxide and hydrogen cyanide emissions from five passenger vehicles.* Science of The Total Environment, 2004. **334–335**(0): p. 125-132.DOI: http://dx.doi.org/10.1016/j.scitotenv.2004.04.061
18. Li, H., et al. *Evaluation of a FTIR Emission Measurement System for Legislated Emissions Using a SI Car. SAE Technical Paper Series 2006-01-3368.* in *Proceedings of Powertrain & Fluid Systems Conference*. 2006. Toronto, Canada: SAE International.DOI: 10.4271/2006-01-3368
19. Xu, Y., L. Yu, and G. Song, *Improved Vehicle-Specific Power Bins for Light-Duty Vehicles in Estimation of Carbon Dioxide Emissions in Beijing.* Transportation Research Record: Journal of the Transportation Research Board, 2010. **2191**(-1): p. 158-165.DOI: 10.3141/2191-20
20. Bielaczyc, P., A. Szczotka, A. Swiatek, and J. Woodburn, *A Comparison of Ammonia Emission Factors from Light-Duty Vehicles Operating on Gasoline, Liquefied Petroleum Gas (LPG) and Compressed Natural Gas (CNG).* SAE Int. J. Fuels Lubr., 2012. **5**(2): p. 751-759.DOI: 10.4271/2012-01-1095

Appendix A: Summary of driving parameters and nitrogen species emissions for all journeys

Journeys	1925_A	1256_A	0746_A	0830_A	1941_B	1316_B	0807_B	0853_B
Av. Velocity (km/hr)	23.09	18.52	17.64	15.34	23.21	19.84	15.33	15.68
Max Velocity (km/hr)	49.42	48.67	44.04	43.48	52.24	49.31	45.48	45.76
Min Velocity (km/hr)	0.00	0.00	0.00	0.00	0.00	0.00	0.00	0.00
Av.Acceleration (m/s2)	0.0001	-0.0034	0.0024	-0.0035	-0.0062	0.0065	0.00	0.00
Max Acceleration (m/s2)	2.29	2.42	2.57	2.17	2.11	2.35	2.65	2.76
Max Deceleration (m/s2)	-1.90	-1.80	-2.35	-1.91	-4.03	-4.30	-2.04	-2.71
Av. VSP (Kw/tonne)	1.56	1.20	1.08	0.96	1.44	1.39	1.01	1.10
Max VSP (Kw/tonne)	20.61	25.76	19.08	16.83	22.96	18.10	19.25	18.47
Min VSP (Kw/tonne)	-13.11	-11.21	-13.49	-12.02	-13.54	-15.01	-14.77	-22.33
Av. VSP+ (Kw/tonne)	3.65	2.89	2.59	2.21	3.21	2.99	2.39	2.02
Av. VSP- (Kw/tonne)	-3.01	-0.74	-2.13	-1.98	-2.48	-2.48	-1.81	-2.45
Power output+ (kWh)	0.83	0.81	0.76	0.75	0.75	0.80	0.80	0.91
Power output- (kWh)	-0.31	-0.30	-0.27	-0.26	-0.25	-0.27	-0.28	-0.35
Total stoppage time (s)	167.00	276.00	281.00	392.00	176.00	235.00	339.00	368.00
stoppage time (%)	21.89	28.93	28.30	34.03	22.80	26.49	29.35	32.74
Cruise%	46.13	36.06	33.30	27.26	47.15	41.38	26.58	28.29
Total fuel consumption (g)	339.30	363.70	380.79	399.75	316.96	370.32	418.99	430.35
Av. fuel consumption (g/s)	0.44	0.38	0.38	0.35	0.41	0.42	0.36	0.38
Idle fuel consumption (g)	41.90	62.81	60.76	84.84	42.56	50.07	83.34	78.45
Idle fuel consumption (%)	12.35	17.27	15.95	21.22	13.43	13.52	19.89	18.23
Journey Av. fuel consumption (g/km)	69.00	74.09	77.53	81.27	63.57	75.46	85.03	87.67
Fuel economy (mile/UKG)	29.55	27.52	26.30	25.09	32.07	27.02	23.98	23.26
Overall thermal efficiency (%)	0.20	0.18	0.16	0.15	0.19	0.18	0.16	0.17
Nitrous oxide N2O (g/km)	0.0003	0.0008	0.0013	0.0011	0.0003	0.0003	0.0007	0.0012
Nitrogen monoxide NO (g/km)	0.04	0.05	0.05	0.03	0.04	0.04	0.02	0.03
Nitrogen dioxide NO2 (g/km)	0.0011	0.0040	0.0111	0.0164	0.0005	0.0051	0.0152	0.0198
Ammonia NH3 (g/km)	0.07	0.07	0.06	0.09	0.05	0.06	0.09	0.08
Hydrogen cyanide HCN (g/km)	0.0005	0.006	0.006	0.012	0.0006	0.008	0.009	0.015
NOx (g/km)	0.07	0.08	0.09	0.06	0.06	0.07	0.05	0.06